

World Journal of *Stem Cells*

World J Stem Cells 2021 November 26; 13(11): 1610-1812



REVIEW

- 1610 Application of dental stem cells in three-dimensional tissue regeneration
Hsiao HY, Nien CY, Hong HH, Cheng MH, Yen TH
- 1625 Priming strategies for controlling stem cell fate: Applications and challenges in dental tissue regeneration
Zhang SY, Ren JY, Yang B
- 1647 Epigenetic regulation of dental pulp stem cells and its potential in regenerative endodontics
Liu Y, Gan L, Cui DX, Yu SH, Pan Y, Zheng LW, Wan M
- 1667 Effects of immune cells on mesenchymal stem cells during fracture healing
Ehnert S, Relja B, Schmidt-Bleek K, Fischer V, Ignatius A, Linnemann C, Rinderknecht H, Huber-Lang M, Kalbitz M, Histing T, Nussler AK
- 1696 Regulation of the mesenchymal stem cell fate by interleukin-17: Implications in osteogenic differentiation
Krstić J, Mojsilović S, Mojsilović SS, Santibanez JF
- 1714 Why stem/progenitor cells lose their regenerative potential
Picerno A, Stasi A, Franzin R, Curci C, di Bari I, Gesualdo L, Sallustio F
- 1733 Nanofat: A therapeutic paradigm in regenerative medicine
Jeyaraman M, Muthu S, Sharma S, Ganta C, Ranjan R, Jha SK

MINIREVIEWS

- 1747 Application of adipose-derived stem cells in treating fibrosis
Li ZJ, Wang LQ, Li YZ, Wang CY, Huang JZ, Yu NZ, Long X

ORIGINAL ARTICLE**Basic Study**

- 1762 Exosomes derived from inflammatory myoblasts promote M1 polarization and break the balance of myoblast proliferation/differentiation
Luo ZW, Sun YY, Lin JR, Qi BJ, Chen JW
- 1783 ARPE-19 conditioned medium promotes neural differentiation of adipose-derived mesenchymal stem cells
Mannino G, Cristaldi M, Giurdanella G, Perrotta RE, Lo Furno D, Giuffrida R, Rusciano D
- 1797 MKK7-mediated phosphorylation of JNKs regulates the proliferation and apoptosis of human spermatogonial stem cells
Huang ZH, Huang C, Ji XR, Zhou WJ, Luo XF, Liu Q, Tang YL, Gong F, Zhu WB

ABOUT COVER

Editorial Board Member of *World Journal of Stem Cells*, Pietro Gentile, MD, PhD, Associate Professor, Surgical Science Department, Plastic and Reconstructive Surgery Unit, University of Rome "Tor Vergata", Rome 00133, Italy. pietrogentile2004@libero.it

AIMS AND SCOPE

The primary aim of *World Journal of Stem Cells (WJSC, World J Stem Cells)* is to provide scholars and readers from various fields of stem cells with a platform to publish high-quality basic and clinical research articles and communicate their research findings online. *WJSC* publishes articles reporting research results obtained in the field of stem cell biology and regenerative medicine, related to the wide range of stem cells including embryonic stem cells, germline stem cells, tissue-specific stem cells, adult stem cells, mesenchymal stromal cells, induced pluripotent stem cells, embryonal carcinoma stem cells, hemangioblasts, lymphoid progenitor cells, etc.

INDEXING/ABSTRACTING

The *WJSC* is now indexed in Science Citation Index Expanded (also known as SciSearch®), Journal Citation Reports/Science Edition, Biological Abstracts, BIOSIS Previews, Scopus, PubMed, and PubMed Central. The 2021 Edition of Journal Citation Reports® cites the 2020 impact factor (IF) for *WJSC* as 5.326; IF without journal self cites: 5.035; 5-year IF: 4.956; Journal Citation Indicator: 0.55; Ranking: 14 among 29 journals in cell and tissue engineering; Quartile category: Q2; Ranking: 72 among 195 journals in cell biology; and Quartile category: Q2. The *WJSC*'s CiteScore for 2020 is 3.1 and Scopus CiteScore rank 2020: Histology is 31/60; Genetics is 205/325; Genetics (clinical) is 64/87; Molecular Biology is 285/382; Cell Biology is 208/279.

RESPONSIBLE EDITORS FOR THIS ISSUE

Production Editor: *Hua-Ge Yu*; Production Department Director: *Yun-Jie Ma*; Editorial Office Director: *Ze-Mao Gong*.

NAME OF JOURNAL

World Journal of Stem Cells

ISSN

ISSN 1948-0210 (online)

LAUNCH DATE

December 31, 2009

FREQUENCY

Monthly

EDITORS-IN-CHIEF

Shengwen Calvin Li, Tong Cao, Carlo Ventura

EDITORIAL BOARD MEMBERS

<https://www.wjgnet.com/1948-0210/editorialboard.htm>

PUBLICATION DATE

November 26, 2021

COPYRIGHT

© 2021 Baishideng Publishing Group Inc

INSTRUCTIONS TO AUTHORS

<https://www.wjgnet.com/bpg/gerinfo/204>

GUIDELINES FOR ETHICS DOCUMENTS

<https://www.wjgnet.com/bpg/GerInfo/287>

GUIDELINES FOR NON-NATIVE SPEAKERS OF ENGLISH

<https://www.wjgnet.com/bpg/gerinfo/240>

PUBLICATION ETHICS

<https://www.wjgnet.com/bpg/GerInfo/288>

PUBLICATION MISCONDUCT

<https://www.wjgnet.com/bpg/gerinfo/208>

ARTICLE PROCESSING CHARGE

<https://www.wjgnet.com/bpg/gerinfo/242>

STEPS FOR SUBMITTING MANUSCRIPTS

<https://www.wjgnet.com/bpg/GerInfo/239>

ONLINE SUBMISSION

<https://www.f6publishing.com>

Basic Study

Exosomes derived from inflammatory myoblasts promote M1 polarization and break the balance of myoblast proliferation/differentiation

Zhi-Wen Luo, Ya-Ying Sun, Jin-Rong Lin, Bei-Jie Qi, Ji-Wu Chen

ORCID number: Zhi-Wen Luo 0000-0002-0524-9951; Ya-Ying Sun 0000-0001-5457-6046; Jin-Rong Lin 0000-0001-5457-6045; Bei-Jie Qi 0000-0002-4041-0050; Ji-Wu Chen 0000-0003-1365-599X.

Author contributions: Chen JW, Luo ZW, and Sun YY designed and performed most of the experiments, analyzed and interpreted the data, and wrote the manuscript; Luo ZW and Lin JR assisted during the acquisition, analysis, and interpretation of data and revised the manuscript; Luo ZW, Qi BJ, and Sun YY assisted with data acquisition and revision of the manuscript; all authors have reviewed and approved the final version of the manuscript; Luo ZW and Sun YY contributed equally to this study.

Institutional animal care and use committee statement: The experiments in this study were approved by Huashan Hospital, Fudan University, No. 20171248A703.

Conflict-of-interest statement: The authors declare that they have no competing interests, and all authors should confirm its accuracy.

Zhi-Wen Luo, Ya-Ying Sun, Jin-Rong Lin, Bei-Jie Qi, Department of Sports Medicine, Huashan Hospital, Fudan University, Shanghai 200040, China

Ji-Wu Chen, Department of Sports Medicine, Shanghai General Hospital, School of Medicine, Shanghai Jiao Tong University, Shanghai, China.

Corresponding author: Ji-Wu Chen, MD, PhD, Academic Research, Chief Doctor, Professor, Department of Sports Medicine, Shanghai General Hospital, School of Medicine, Shanghai Jiao Tong University, Shanghai, China. jeevechen@gmail.com

Abstract

BACKGROUND

Acute muscle injuries are one of the most common injuries in sports. Severely injured muscles are prone to re-injury due to fibrotic scar formation caused by prolonged inflammation. How to regulate inflammation and suppress fibrosis is the focus of promoting muscle healing. Recent studies have found that myoblasts and macrophages play important roles in the inflammatory phase following muscle injury; however, the crosstalk between these two types of cells in the inflammatory environment, particularly the exosome-related mechanisms, had not been well studied.

AIM

To evaluate the effects of exosomes from inflammatory C2C12 myoblasts (IF-C2C12-Exos) on macrophage polarization and myoblast proliferation/differentiation.

METHODS

A model of inflammation was established *in vitro* by lipopolysaccharide stimulation of myoblasts. C2C12-Exos were isolated and purified from the supernatant of myoblasts by gradient centrifugation. Multiple methods were used to identify the exosomes. Gradient concentrations of IF-C2C12-Exos were added to normal macrophages and myoblasts. PKH67 fluorescence tracing was used to identify the interaction between exosomes and cells. Microscopic morphology, Giemsa stain, and immunofluorescence were carried out for histological analysis. Additionally, ELISA assays, flow cytometry, and western blot were conducted to analyze molecular changes. Moreover, myogenic proliferation was assessed by the BrdU

Data sharing statement: The datasets used and/or analyzed during the current study are available from the corresponding author on reasonable request.

ARRIVE guidelines statement: The authors have read the ARRIVE Guidelines, and the manuscript was prepared and revised according to the ARRIVE Guidelines.

Supported by National Natural Science Foundation of China, No. 81772419 and No. 81972062.

Country/Territory of origin: China

Specialty type: Cell and tissue engineering

Provenance and peer review: Invited article; Externally peer reviewed.

Peer-review report's scientific quality classification

Grade A (Excellent): 0
Grade B (Very good): B, B, B
Grade C (Good): 0
Grade D (Fair): 0
Grade E (Poor): E

Open-Access: This article is an open-access article that was selected by an in-house editor and fully peer-reviewed by external reviewers. It is distributed in accordance with the Creative Commons Attribution NonCommercial (CC BY-NC 4.0) license, which permits others to distribute, remix, adapt, build upon this work non-commercially, and license their derivative works on different terms, provided the original work is properly cited and the use is non-commercial. See: <http://creativecommons.org/licenses/by-nc/4.0/>

Received: May 1, 2021

Peer-review started: May 1, 2021

First decision: June 16, 2021

Revised: June 28, 2021

Accepted: September 2, 2021

Article in press: September 2, 2021

Published online: November 26, 2021

P-Reviewer: Pethe P, Wang Z,

test, scratch assay, and CCK-8 assay.

RESULTS

We found that the PKH-67-marked C2C12-Exos can be endocytosed by both macrophages and myoblasts. IF-C2C12-Exos induced M1 macrophage polarization and suppressed the M2 phenotype *in vitro*. In addition, these exosomes also stimulated the inflammatory reactions of macrophages. Further-more, we demonstrated that IF-C2C12-Exos disrupted the balance of myoblast proliferation/differentiation, leading to enhanced proliferation and suppressed fibrogenic/myogenic differentiation.

CONCLUSION

IF-C2C12-Exos can induce M1 polarization, resulting in a sustained and aggravated inflammatory environment that impairs myoblast differentiation, and leads to enhanced myogenic proliferation. These results demonstrate why prolonged inflammation occurs after acute muscle injury and provide a new target for the regulation of muscle regeneration.

Key Words: C2C12 myoblast; Exosomes; Macrophage polarization; Inflammation; Differentiation; Proliferation

©The Author(s) 2021. Published by Baishideng Publishing Group Inc. All rights reserved.

Core Tip: For successful muscle regeneration, macrophage polarization and myogenesis should be supported by an appropriate combination of cells and their signals. As the communication between myoblasts and macrophages within the inflammatory environment is unknown, we aimed to evaluate the effects of IF-C2C12-Exos on macrophage polarization and myoblast proliferation/differentiation. We found that IF-C2C12-Exos could induce M1 polarization, resulting in a sustained and exacerbated inflammatory environment, impaired myoblast fibrogenic/myogenic differentiation, and led to abnormal myogenic proliferation. These results indicate a potential mechanism for the development of long-term inflammation following acute muscle injury, but further preclinical evaluations targeting IF-C2C12-Exos in animal models are necessary.

Citation: Luo ZW, Sun YY, Lin JR, Qi BJ, Chen JW. Exosomes derived from inflammatory myoblasts promote M1 polarization and break the balance of myoblast proliferation/differentiation. *World J Stem Cells* 2021; 13(11): 1762-1782

URL: <https://www.wjgnet.com/1948-0210/full/v13/i11/1762.htm>

DOI: <https://dx.doi.org/10.4252/wjsc.v13.i11.1762>

INTRODUCTION

More than half of sports injuries in athletes have been reported to be related to muscle damage[1]. In addition to promoting muscle regeneration, preventing scar formation is a key factor in the healing of injured muscle[2-4], as localized fibrotic tissue can lead to susceptibility to re-injury of injured muscles[5,6].

Skeletal muscle fibrosis is related to excessive local inflammation and myoblast fibrogenic differentiation in the early stage after injury[7-11]. During the general inflammatory process following injury, M1 macrophages (classically activated) are recruited and lead to further muscle damage[12], which are then substituted by M2 macrophages (alternatively activated) to promote muscle regeneration and differentiation[13]. Sometimes, M2 polarization is suppressed by the excessive inflammatory conditions that follow acute muscle injury[14,15]. Given the timing of the appearance of M1 coupled with that of myoblasts within 1-3 d after muscle injury[12,16], we suppose that myoblasts may be able to influence the shift from M1 macrophages to M2 subtype. Periodontal ligament stem cells and adipocytes within the inflammatory environment have been reported to inhibit the M2 polarization of macrophages through exosomes[17,18]. Many species of living cells such as myoblasts secrete

Zhang Q

S-Editor: Fan JR**L-Editor:** Webster JR**P-Editor:** Yu HG

exosomes that can be transported and regulate the essential cell activities such as proliferation and differentiation of neighboring cells[19-22]. Therefore, we speculated that in the prolonged inflammatory micro-environment of injured muscle, myoblasts might promote M1 macrophage polarization and suppress M2 phenotype through exosomes.

Additionally, Guescini *et al*[23] reported that exosomes derived from myotubes can influence the balance of proliferation and differentiation of normal myoblasts after H₂O₂ administration, suggesting that the C2C12-Exos could also regulate muscle healing through self-control[23]. In our previous studies, we found that myoblasts could be converted to myofibroblasts after muscle injury due to its intracellular signals including lncRNA-MFAT1/H19, miR-122-5p/25-3p, and transforming growth factor-β (TGF-β)/SMAD[24-26], which may contribute to muscle fibrosis. Therefore, it is worth investigating whether C2C12-Exos could influence the fibrogenic/myogenic differentiation and proliferation of normal myoblasts.

In this study, we isolated C2C12-Exos from myoblasts within an inflammatory environment, tested their functions, and investigated the potential underlying mechanisms of the effects of C2C12-Exos on the immunomodulation of macrophages and myoblasts proliferation/differentiation *in vitro*.

MATERIALS AND METHODS

Cell culture

C2C12 myoblasts (murine cell line), purchased from ScienCell Research Laboratories, were maintained in high glucose Dulbecco's modified eagle medium (DMEM) (HyClone) with 10% fetal bovine serum (FBS) and 0.5 mL of penicillin/streptomycin solution (#0503; ScienCell Research Laboratories) in a humidified incubator at 37°C and 5% CO₂ atmosphere. Muscle differentiation was induced using 2% horse serum (ThermoFisher) for C2C12. Lipopolysaccharide (LPS), at a concentration of 1000 ng/mL was used to induce an inflammatory environment for C2C12. The medium was then washed three times to remove all the LPS and a fresh exosome-depleted medium was added. C2C12 conditioned media (C2C12-CM) were collected using a 1 mL pipette and added into 50 mL tubes after 24 h incubation. The media were then kept at -80°C before use. Exosomes from C2C12 myoblasts (C2C12-Exos) were extracted by the following steps.

RAW264.7 cells (mouse leukemia cells of monocyte-macrophage), purchased from the American Type Culture Collection, were cultured in DMEM containing 10% FBS and 0.5 mL of penicillin/streptomycin solution in a humidified incubator at 37°C and 5% CO₂ atmosphere.

Isolation and identification of C2C12-Exos

The extraction procedure for C2C12-Exos was based on a previous method[27]. 50 mL conditioned culture medium containing 5 mL exosome-free FBS (Exosome-depleted FBS, Gibco), and 0.5 mL of penicillin/streptomycin solution were used to culture C2C12s for 48 h. After the C2C12s had grown to more than 90% confluence, the cells were treated with LPS for 1 d. Then, fresh culture medium was added, and the cells were kept quiescent for 24 h, and then all the supernatant was collected. After that, all media were subjected to sequential centrifugation (Optima XPN-100 ultracentrifuge; Beckman Coulter SW 41 Ti rotor) at 10000 ×g for 35 min (to remove the cell debris) and then at 100000 ×g for 70 min. After this step, at 100000 ×g for 70 min the precipitate was washed twice with phosphate-buffered saline (PBS). The C2C12-Exos were resuspended in PBS and stored at -80°C prior to processing.

To observe the morphology of exosomes, C2C12-Exos were assessed directly under transmission electron microscopy (Tecnai G2 Spirit, Tecnai) and scanning electron microscopy (SEM, MIRA3 FEG-SEM, TESCAN). The SEM procedures were based on a previous study[28]. Generally, 100 μL of the exosome suspension was frozen overnight in the refrigerator and then transferred to a vacuum dryer for lyophilization. An appropriate amount of freezing glue was applied to the sample table and then the exosome lyophilized powder was spread onto the sample table. The samples were then coated with gold with an ion sputterer and observed under the microscope.

To assess the absolute size distribution of C2C12-Exos, they were analyzed using a NanoSight NS300 (Malvern, United Kingdom). The particles were automatically tracked and sized using nanoparticle tracking analysis (NTA) based on Brownian motion and diffusion coefficients.

Table 1 Primary antibodies used in the experiment

Antibody	Source	Catalog No.	Type	Dilution	M.W. (kD)
CD63	Affinity	AF5117	Rabbit mAb	1:1000(W.B.)	47
CD9	Affinity	AF5139	Rabbit mAb	1:2000(W.B.)	23
Alix	Affinity	ab275377AF0184	Rabbit mAb	1:2000(W.B.)	95
HSP60	Affinity	AF0199	Rabbit mAb	1:2000(W.B.)	60
iNOS	Affinity		Rabbit mAb	1:1000(W.B.)	130
ARG1	Affinity	DF6657	Rabbit mAb	1:1000(W.B.)	35
CD86	Abcam	ab220188	Rabbit mAb	1:1000(W.B.) 1:100(IF)	38
CD86 PE	eBioscience	12-0862-81	Rat mAb	0.125 µg/test	(Flow Cyt)
CD206	Affinity	DF4149	Rabbit mAb	1:1000(W.B.)	120
CD206	Abcam	ab64693	Rabbit mAb	1:500(IF)	
	eBioscience	17-1631-80	Rat mAb	0.25 µg/test	(Flow Cyt)
CD163APC	Abcam	ab51263	Mouse mAb	1:1000(W.B.)	227
MYHC				1:500(IF)	
MyoD1	Affinity	AF7733	Rabbit mAb	1:1000(W.B.)	60
MyoD1	Proteintech	18943-1-AP	Rabbit PAb	1:200(IF)	
MyoG	Abcam	ab1835	Mouse mAb	1:1000(W.B.)	25
Collage 1	Affinity	AF7001	Rabbit mAb	1:1000(W.B.)	140
α-SMA	Affinity	AF1032	Rabbit mAb	1:1000(W.B.)	42
Tubulin	Affinity	T0023	Mouse mAb	1:1000(W.B.)	55
GAPDH	Affinity	AF7021	Rabbit mAb	1:1000(W.B.)	37
F4/80 APC	eBioscience	47-4801-80	Rat mAb	0.125 µg/test	(Flow Cyt)

α-SMA: α-smooth muscle actin.

To identify the surface markers of C2C12-Exos, exosomes were assessed by flow cytometry analysis using a commercially Exo-Flow capture kit, including CD9, CD47, CD63, and CD81 flow antibodies (System Biosciences, CA, United States). These procedures were *per* the published studies[29].

Additionally, the C2C12-Exos were identified by Western blotting with anti-CD63, anti-CD9, anti-Alix, and anti-HSP60 antibodies (purchased from Abcam or Affinity) (Table 1).

Cell intervention

C2C12 and RAW264.7 cells were incubated at 1×10^7 cells in 10 cm plates and divided into groups according to different IF-C2C12-Exos concentrations or conditioned medium. After 24 or 48 h of incubation, macrophages were collected for flow cytometry/western blot or fixation to assess histological changes. After 48 h of treatment with high concentrations of IF-C2C12-Exos, macrophages were collected in conditioned medium. In this study, we defined this as M1CM, meaning that the macrophages in the medium were more of the M1 subtype rather than M2 or M0 macrophages. In addition, C2C12 cells were incubated with exosomes for 24 h for further experiments, including proliferation and differentiation (Figure 1).

Exosome labeling with PKH67

Isolated C2C12-Exos were labeled with PKH67 (a Green Fluorescent Labeling Kit (Sigma, Aldrich, MINI67-1KT)), and the procedures followed the manufacturer's protocol. C2C12-Exos or PBS were stained with PKH67 dye in 500 µL of Diluent C solution for 5 min at room temperature. After that, 1 mL 1% BSA was used to stop the labeling process. Then the re-purified exosomes underwent ultracentrifugation with a

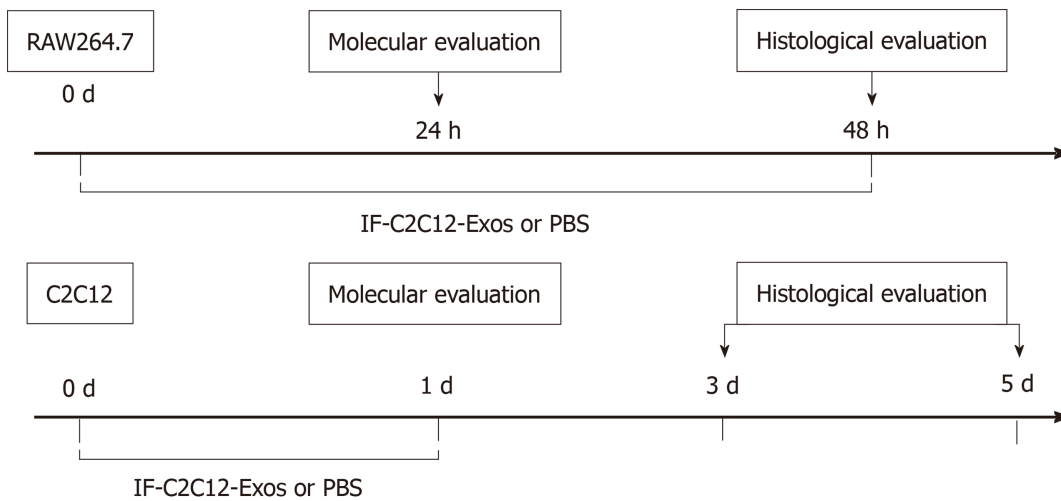


Figure 1 Experimental design for both the *in vitro* and *in vivo* studies. IF-C2C12-Exos, Myoblast-derived exosomes within the inflammatory environment; Molecular evaluation included Western Blot, ELISA, immunofluorescence, and flow cytometry. Histological evaluation included immunofluorescence and electron microscopy. PBS: Phosphate-buffered saline.

PBS rinse for 30 min. The labeled PBS or C2C12-Exos were co-incubated with C2C12 cells and macrophages (M0) for 12 h at 37°C, in a 5% CO₂ cell incubator. After incubation, the culture medium was discarded and the cells were washed with PBS three times. Cells were fixed with 4% PFA and nuclei were counterstained with DAPI for 5 min. The uptake of labeled exosomes by C2C12 and macrophages was observed by a fluorescence microscope (ECHO Revolve, United States). Six random images of cells were taken, and PKH-67 positive cells were counted. The total number of cells was calculated using the DAPI staining method. The positive rate of PKH-67 = PKH-67 positive cells/total number of cells.

Histological analysis

Macrophage differentiation and morphology: M0 macrophages were incubated with different concentrations of IF-C2C12-Exos for 2 d (1×10^9 , 1×10^{10} , 2×10^{10} /medium). Macrophage cultures were then viewed directly under a microscope (ECHO Revolve, United States).

Immunofluorescence staining: To examine the expression and location of target proteins, cells were immunofluorescently stained as previously described[30]. The primary antibodies used were anti-CD86, anti-CD206, anti-MYHC, anti-iNOS, and anti-MyoD1. DAPI was used to locate the nuclei of the cells. Images were taken using fluorescence microscopy (ECHO Revolve, United States).

Giemsa stain: C2C12 cells were washed with PBS, fixed with 4% PFA for 10 min, and rinsed three times with fresh PBS for 5 min each time. The fixed cells were then incubated with Giemsa stain (Phygene, China) for 50 min. Cells were rinsed with tap water for 3 min and then photographed using an inverted microscope. Three images were taken randomly at 200 × magnification for each well. The numbers of total and fused cell nuclei were counted. Cell counting was performed using ImageJ. The fusion rate was defined as the percentage of total nuclei being in myotubes/total nuclei of C2C12 cells. The diameter and length of the myotube were analyzed by Image-Pro Plus 7.0.

Flow cytometry for M1/M2

Flow cytometry was performed using anti-CD86-PE, anti-CD163-APC, and anti-F4/80-FITC (Thermo/eBio). The percentage of CD86 +/CD163 +/F4/80 + cell population (macrophages) was evaluated using Cytomics™ FC 500 (Beckman Coulter). In detail, different groups of macrophages were collected with flow cytometry staining buffer (eBioscience). Then, 2 μL antibody was added to each 100 μL of cell suspension for 60 min at 4°C in the dark. Then, 5 mL staining buffer was put into each tube and the cell suspension was centrifuged for 5 min (500 ×g, 4°C). The washing procedures were repeated three times. Finally, the cell precipitation was re-suspended in 200 μL PBS for flow cytometry analysis.

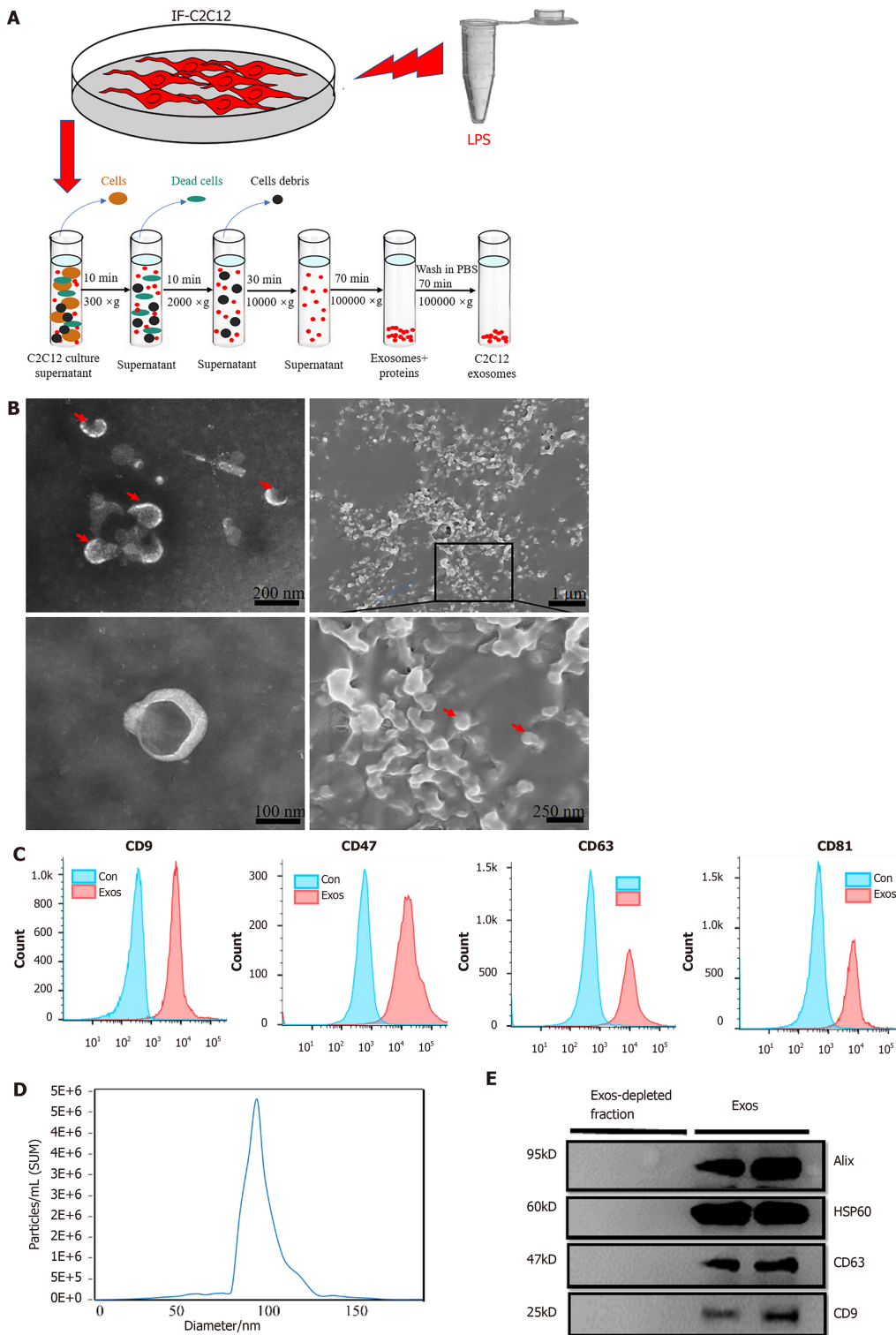


Figure 2 Purification, isolation, and characterization of C2C12-Exos. A: Flowchart of C2C12-Exos purification based on differential ultra-centrifugation. Lipopolysaccharide, 1000 ng/mL for 1 d; B: The morphology of C2C12-Exos was observed by transmission electron microscopy (left) and scanning electron microscopy (right). The red arrows indicate representative exosomes; C: Representative flow cytometry plots showing the phenotypes of exosome markers, including CD9, CD47, CD63, and CD81; D: The particle size distribution of C2C12-Exos was analyzed by the qNano platform; E: Western blotting showed the presence of exosomal markers, including CD63, HSP60, Alix, and CD9. The four lanes represent different exosomal proteins and deproteinized supernatants extracted from the two independent conditioned media. LPS: Lipopolysaccharide.

Western blot

Protein was extracted and analyzed using an established method[31]. Briefly, total protein from C2C12 was collected using RIPA lysis buffer (R0010; Solarbio, Beijing, China) with phenylmethanesulfonyl fluoride (PMSF; Solarbio, Beijing, China). Protein concentrations were measured using a BCA Protein Assay Kit (Beyotime Biotech-

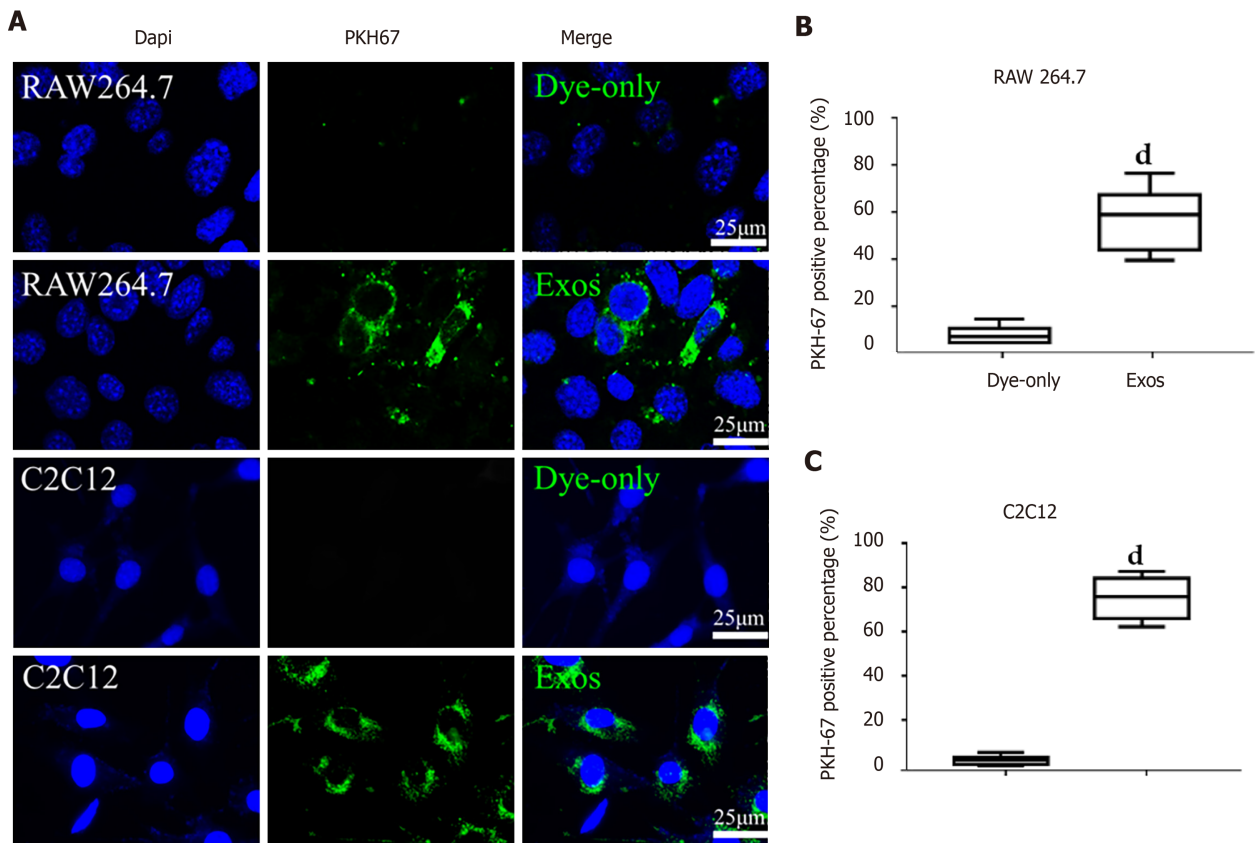


Figure 3 C2C12-Exos were taken up by C2C12 and RAW264.7 cells *in vitro*. A: Representative images of the uptake of PKH67-labeled exosomes (green) by RAW264.7 cells or C2C12 cells (DAPI blue) and fluorescence uptake by negative control samples. Dye-only, only PKH67 incubated with RAW264.7 cells and C2C12 cells; scale bar = 25 μ m; B and C: The percentage of PKH67 positive cells in RAW264.7 or C2C12 is presented. ^d $P < 0.0001$, $n = 6$.

nology, Shanghai, China). Next, 10 μ g protein samples from each group were separated by 10% SDS-PAGE. Afterward, they were transferred to nitrocellulose membranes. 5% non-fat milk dissolved in Tris-buffered saline containing Tween-20 was utilized to block the blots before applying primary antibodies overnight at 4°C. Anti-CD206, anti-Arginase 1, anti-iNOS, anti-CD86, anti-MYHC, anti-MyoD1, anti-MyoG, anti-Col 1, anti- α -SM, anti- β -Tubulin, and anti-GAPDH antibodies were applied as primary antibodies (Table 1). Each group contained 4 protein samples for calculation ($n = 4$).

C2C12 proliferation and migration

BrdU test: The proliferation of C2C12 cells was determined using the 5-Bromo-2'-deoxyuridine (BrdU) incorporation assay kit (Cell Signaling Technology, MA, United States) according to the manufacturer's instructions. Briefly, cells were seeded into a 6-well plate with 1×10^6 cells *per well*. BrdU solution was added into each well 3 h prior to IF-C2C12-Exos treatment. Cell proliferation was evaluated using the average number of BrdU + cells *per view*.

Scratch assay: To assess the cell migration properties of C2C12, an *in vitro* scratch assay was performed by scratching a straight line in the middle of cells cultured for 24 h. Then, different concentrations of IF-C2C12-Exos were applied for 24 h and observed under an inverted microscope. Cell migration ability was evaluated by the percentage of wound-healing rate (distance migrated/ original wound distance $\times 100\%$).

CCK-8 assay: The Cell Counting Kit-8 (CCK-8, Beyotime Biotechnology, Shanghai, China) assay was used to assess the viability of C2C12 cells after IF-C2C12-Exos treatment. The general procedure followed that outlined in a previous study[32]. Briefly, primary cells were seeded into a 96-well plate (Thermo Fisher Scientific, MA, United States) with 1×10^3 cells *per well* and treated with IF-C2C12-Exos for 24 h. Next, CCK-8 solution (10 μ L) was applied to each well, and the plate was incubated for 2 h and the absorbance of each well was measured at 450 nm using a Microplate Reader (Bio-Rad, Hercules, CA, United States). Cell viability was evaluated by average absorbance of the IF-C2C12-Exos treatment group/absorbance of control group \times

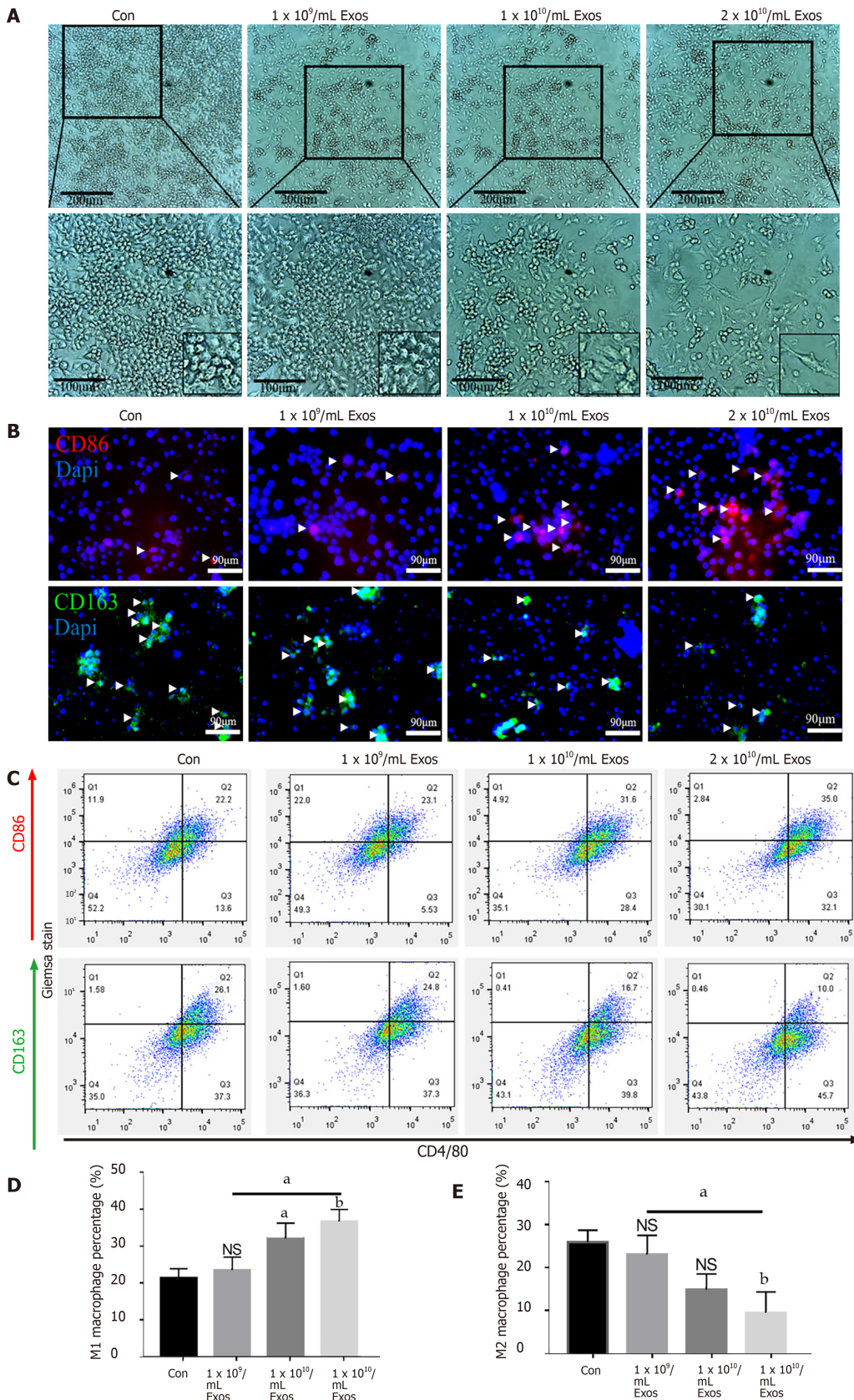


Figure 4 IF-C2C12-Exos induced M1 macrophage polarization *in vitro*. A: Images of macrophages cultured with different concentrations of C2C12-Exos for 2 d (1×10^9 , 1×10^{10} , 2×10^{10} /medium). Scale bar = 200 μ m or 100 μ m; B: Immunofluorescence localization of CD86 (red), marker of M1 and CD206 (green), marker of M2 after culture with different concentrations of C2C12-Exos for 2 d. Scale bar = 90 μ m. Arrows indicate CD206 or CD86 positive cells; C: Representative flow cytometry plots showing the percentages of M1 (CD86 + CD4/80+) and M2 (CD163 + CD4/80+) phenotype in macrophages after culture with different concentrations of C2C12-Exos for 24 h; D: Quantification of flow cytometry data ($n = 3$); E: M2 macrophages percentage. Data are presented as mean \pm SD. ^a $P < 0.05$; ^b $P < 0.01$. NS: Not significant.

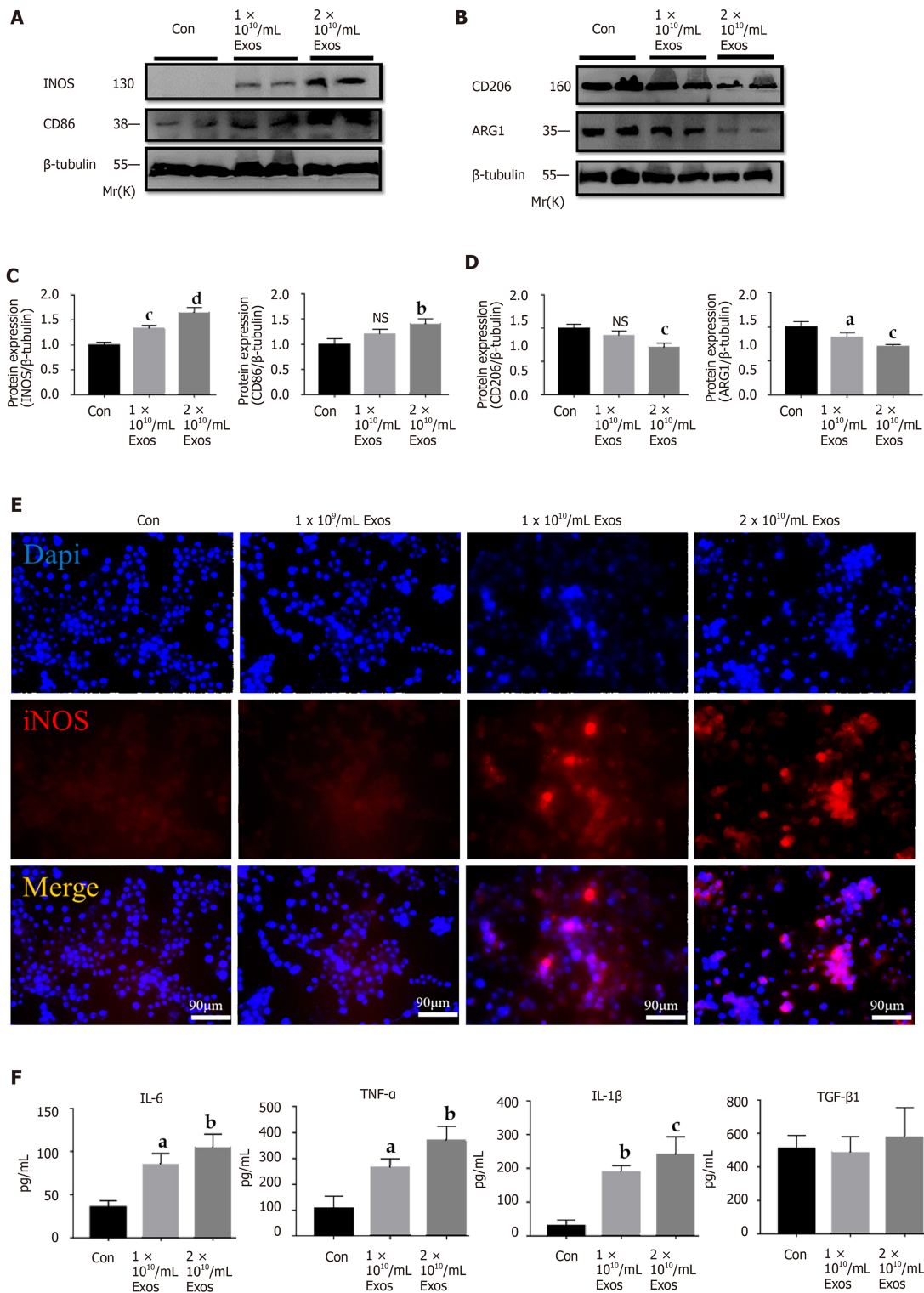


Figure 5 IF-C2C12-Exos induced inflammatory reactions of macrophages *in vitro*. A-D: iNOS, CD86, CD206, and Arg1 protein levels in macrophages were determined by western blot after culturing with different concentrations of C2C12-Exos for 24 h (1 × 10¹⁰, 2 × 10¹⁰/medium). (n = 4). Data are expressed as the mean ± SD. ^aP < 0.05, ^bP < 0.01, ^cP < 0.001, ^dP < 0.0001; E: Immunofluorescence localization and relative expression of iNOS, a marker of inflammatory level, in macrophage medium after culture with different concentrations of C2C12-Exos for 24 h. Scale bar = 90 μm; F: The concentration of cytokine interleukin (IL)-6, transforming growth factor-β, tumor necrosis factor-α, and IL-1β in supernatants of macrophage cells after culture with IF-C2C12-Exos or phosphate-buffered saline for 24 h measured by ELISA (n = 3). ^aP < 0.05, ^bP < 0.01, ^cP < 0.001. PBS: Phosphate-buffered saline. IL: Interleukin; TGF-β: Transforming growth factor-β; TNF-α: Tumor necrosis factor-α; NS: Not significant.

100%.

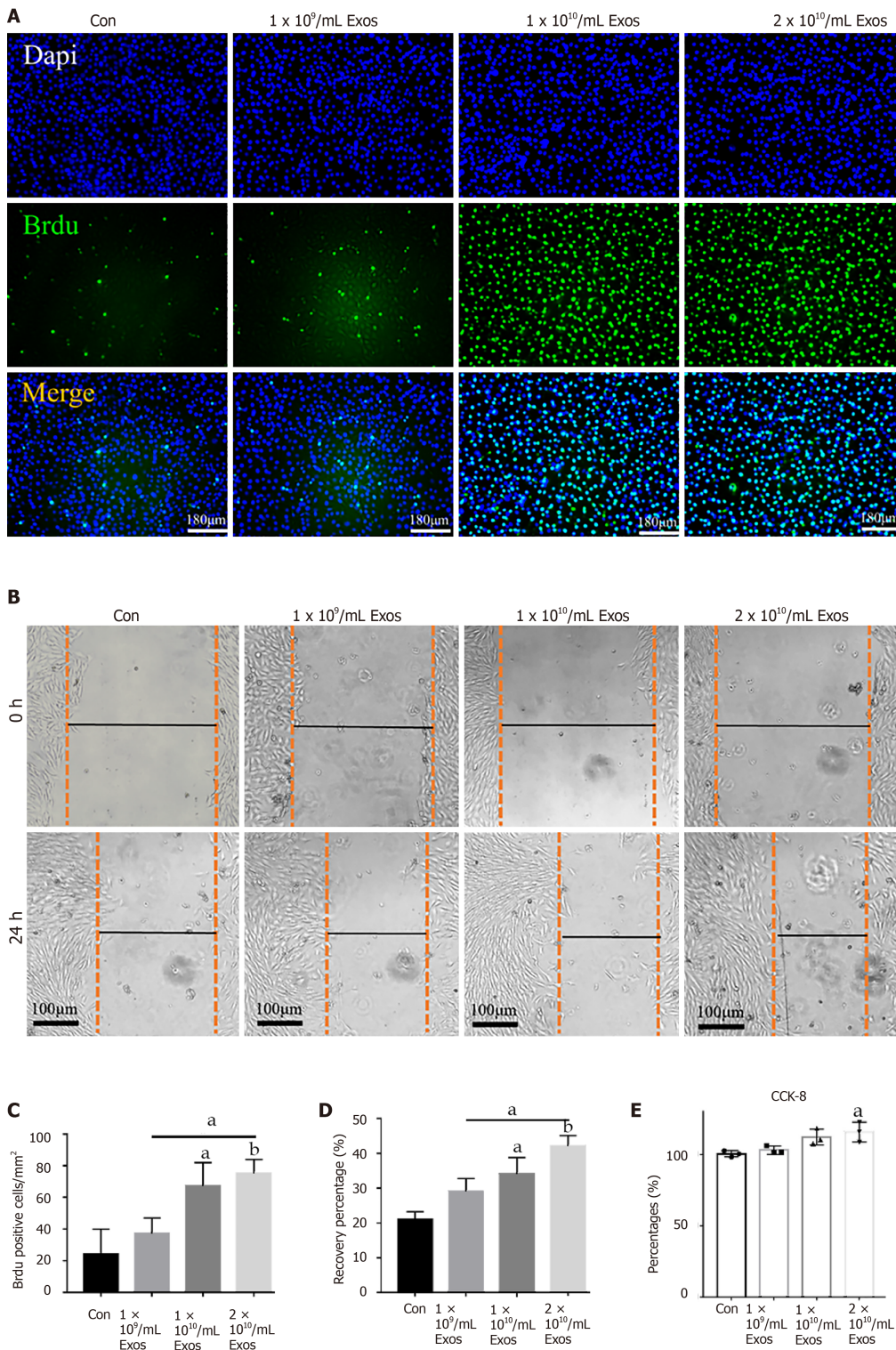


Figure 6 IF-C2C12-Exos stimulated C2C12 proliferation *in vitro*. A: Cell proliferation ability of C2C12 was determined using the BrdU incorporation assay after 24 h IF-C2C12-Exos incubation. Green signal = BrdU. Scale bar = 180 μ m; B: The cell migration ability of C2C12 was determined by the wound-healing assay after 24 h IF-C2C12-Exos incubation; C and D: Quantification of BrdU and wound-healing data ($n = 3$). Data are presented as mean \pm SD. ^a $P < 0.05$, ^b $P < 0.01$; E: Cell proliferation ability of C2C12 was further determined using the CCK-8 assay. Data are presented as mean \pm SD. ^a $P < 0.05$.

Enzyme-linked immunosorbent assay

Enzyme-linked immunosorbent assay (ELISA) kits, including interleukin (IL)-6, IL-1 β , TGF- β , and tumor necrosis factor- α (TNF- α), were purchased from Laizee (LEM060-2, LEM012-2, LEM822-2, LEM810-2). The protocol followed previous studies[33]. Cell supernatants were collected from each group and the kits were then utilized following the manufacturer's instructions. In detail, 100 μ L of samples and standard samples were added to the corresponding well, the plates were sealed and incubated at room

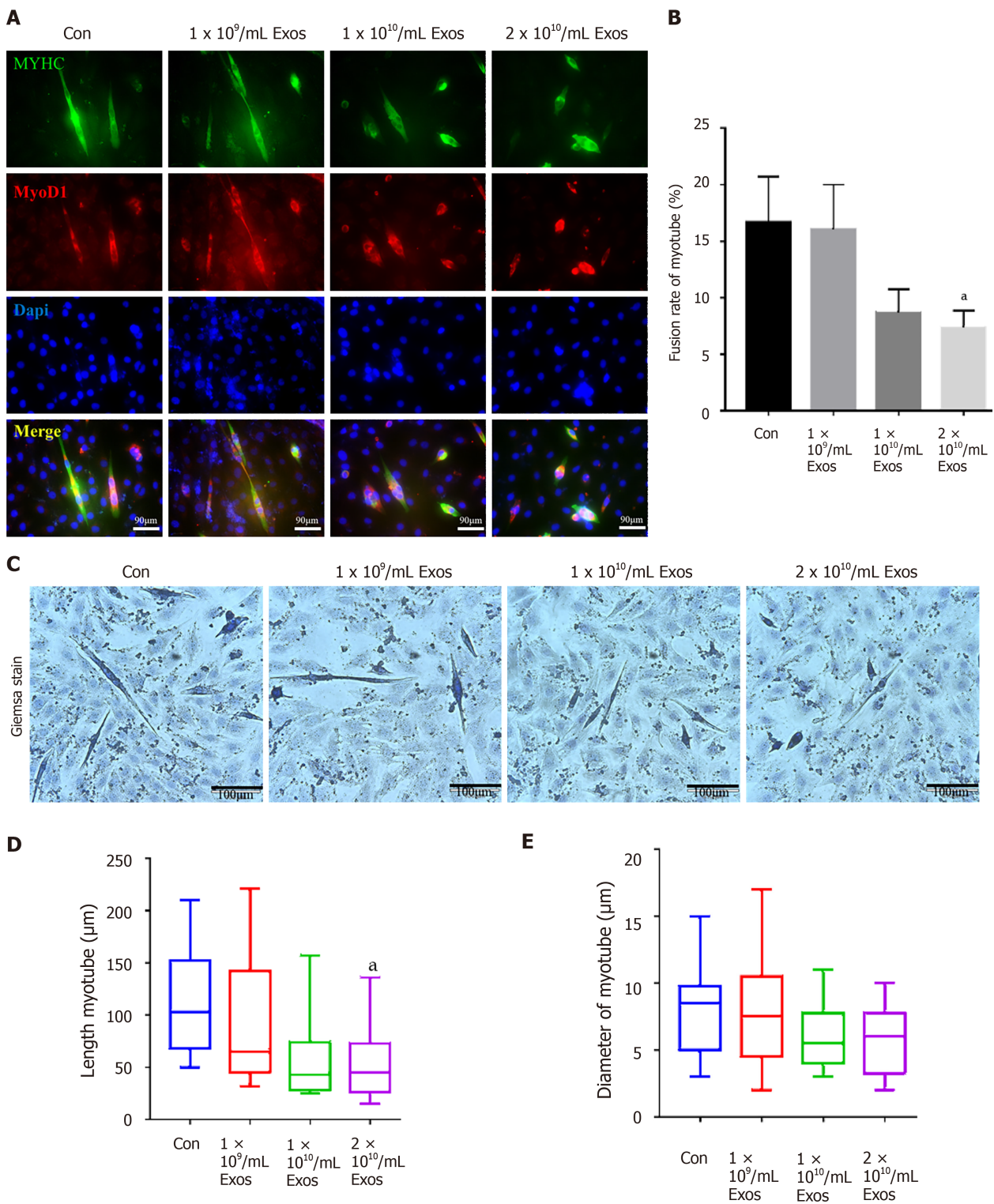


Figure 7 IF-C2C12-Exos impaired early C2C12 muscle differentiation *in vitro*. A: Immunofluorescence was used to detect relative expression and distribution of MYHC and MyoD1 on day 2 after different treatments. Green, red, and blue signals represent MYHC, MyoD1, and nucleus, respectively. Scale bar = 90 μm; B, D and E: Quantification of myotube length, diameter, and fusion rate. Data are presented as mean ± SD. *n* = 12 or 3. ^a*P* < 0.05; C: Representative images of myotube after culture with different concentrations of IF-C2C12-Exosomes for 24 h by Giemsa staining (2 d 2% horse-serum incubation). Scale bar = 100 μm.

temperature for 2 h. The samples were then discarded and the plates were washed 5 times with 300 μL of wash and drained on paper. Then 100 μL avidin HRP solution was added to each well, the plate was sealed, and incubated at room temperature for 30 min. The washing procedure was repeated. Next, 100 μL TMB solution was added to each well, the plate was sealed, and incubated for 15 min at room temperature. Finally, 50 μL of terminator solution was added to terminate the reaction and the plate was analyzed at 450 nm.

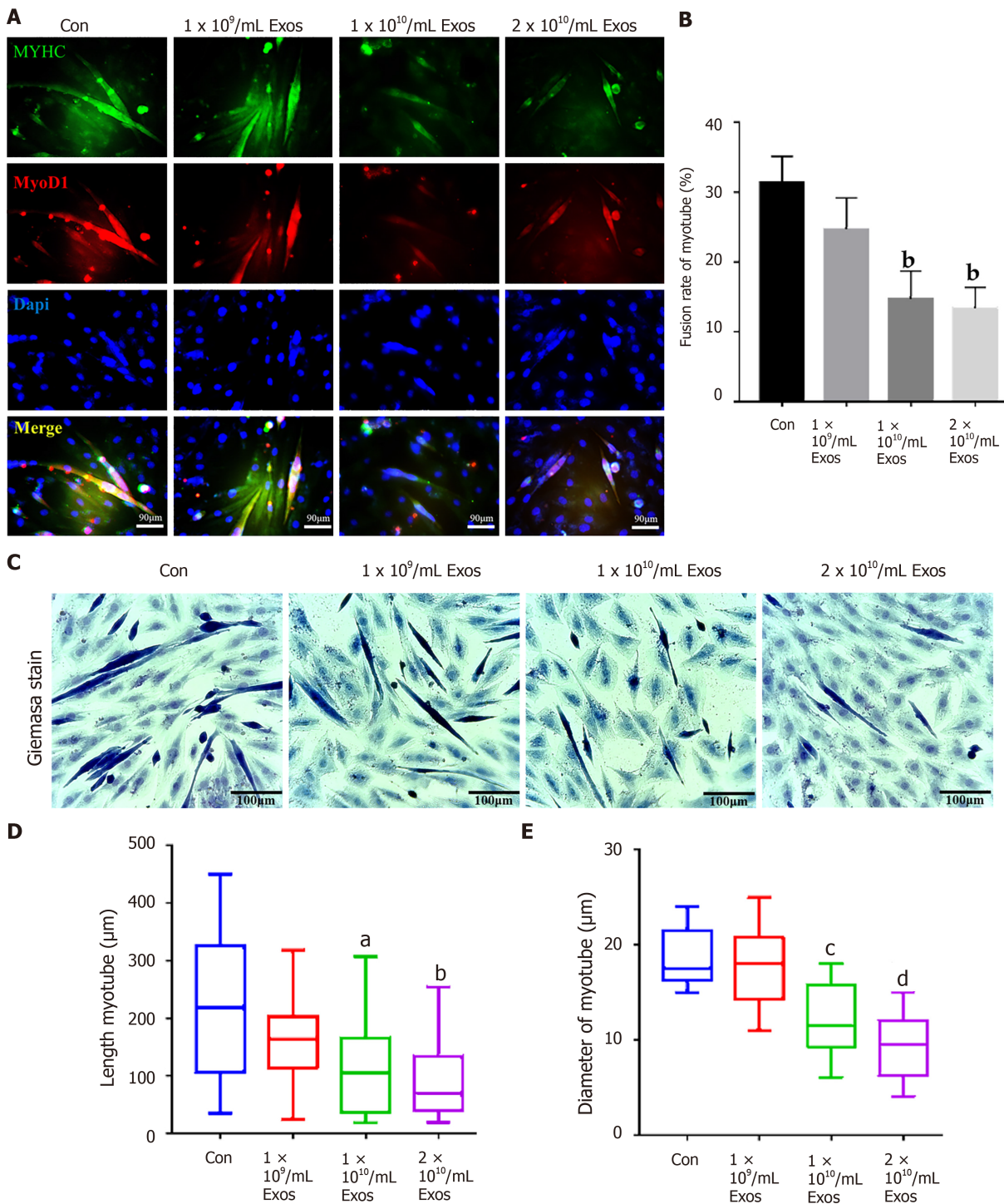


Figure 8 IF-C2C12 Exos impaired C2C12 muscle differentiation *in vitro*. A: Immunofluorescence was used to detect relative expression and distribution of MYHC and MyoD1 on day 4 after different treatments. Green, red, and blue signals represent MYHC, MyoD1, and nucleus, respectively. Scale bar = 90 μm; B, D and E: Quantification of myotube length, diameter, and fusion rate. Data are presented as mean ± SD. $n = 12$ or 3 . ^a $P < 0.05$, ^b $P < 0.01$, ^c $P < 0.001$, ^d $P < 0.0001$; C: Representative images of myotube after culture with different concentrations of IF-C2C12-Exosomes for 24 h by Giemsa staining (4 d 2% horse-serum incubation). Scale bar = 100 μmT.

Statistical analysis

All experiments were performed at least three times. Data were analyzed using GraphPad Prism 7.0 (GraphPad Software, La Jolla, United States) and presented as the mean ± SD. Significance was typically analyzed by Student's *t*-test, or one-way ANOVA followed by post hoc LSD test. $P < 0.05$ was regarded as significant. ^a $P < 0.05$; ^b $P < 0.01$; ^c $P < 0.001$ and ^d $P < 0.0001$.

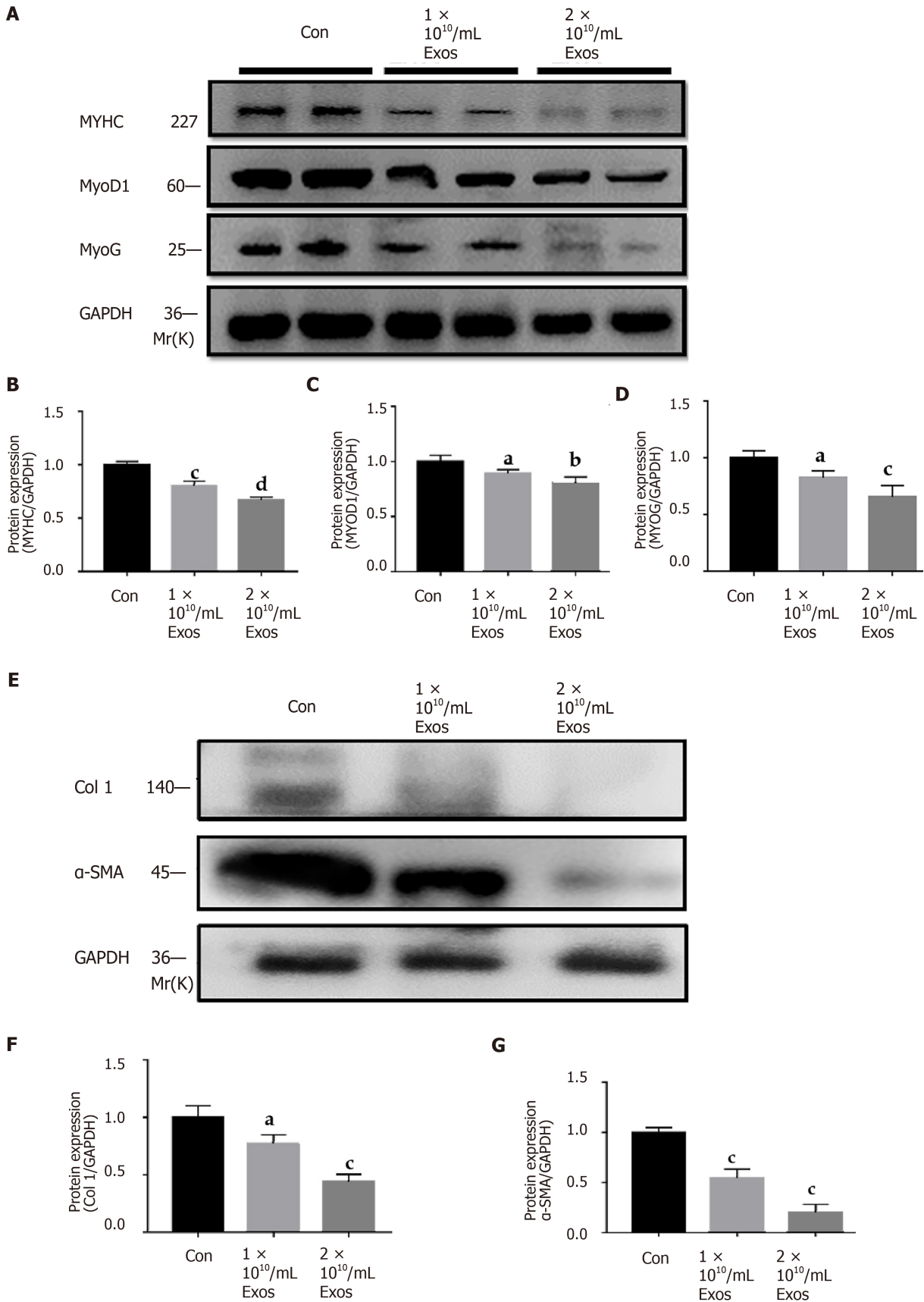


Figure 9 IF-C2C12 Exos down-regulated C2C12 fibrogenic/myogenic differentiation-related proteins *in vitro*. A-D: MYHC, MYOD1, and MYOG protein levels in C2C12 medium were determined by western blot after incubation with different concentrations of C2C12-Exos for 24 h (1×10^9 , 1×10^{10} , 2×10^{10} /medium) ($n = 4$); E-G: Col 1 and α -smooth muscle actin. Data are presented as mean \pm SD. ^a $P < 0.05$, ^b $P < 0.01$, ^c $P < 0.001$, ^d $P < 0.0001$. α -SMA: α -smooth muscle actin.

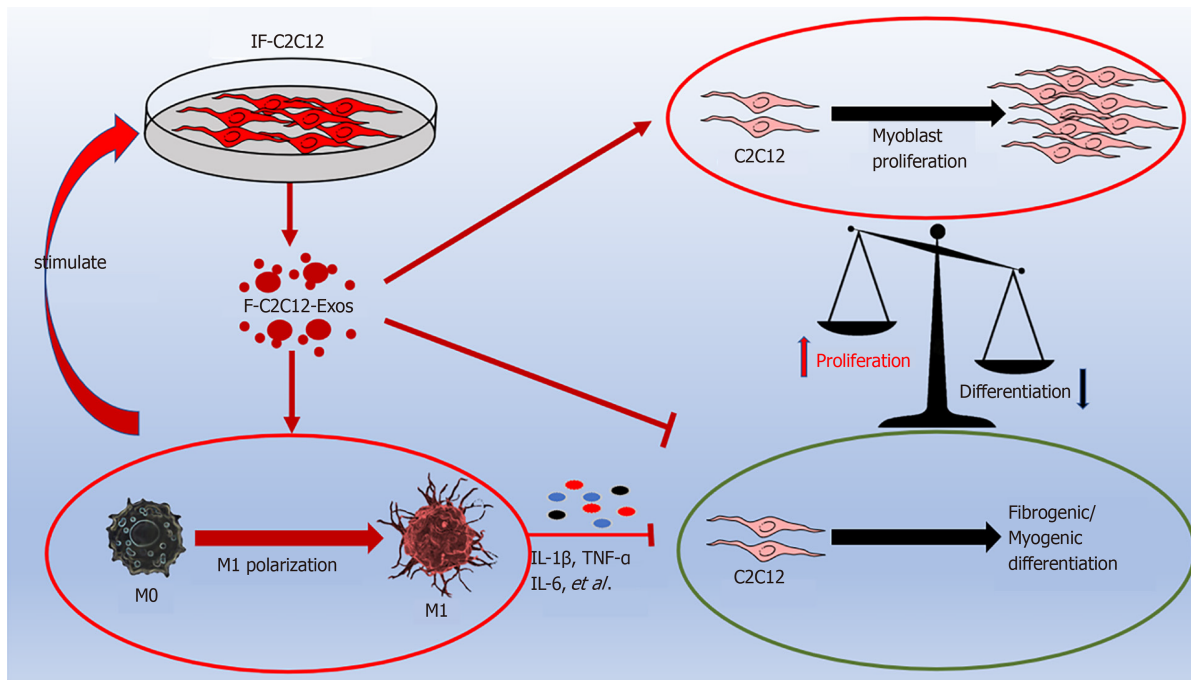


Figure 10 Graphic abstract. IF-C2C12-Exos promoted M1 macrophage polarization and myoblast proliferation, and inhibited myoblast fibrogenic/myogenic differentiation. IL: Interleukin; TNF- α : Tumor necrosis factor- α .

C2C12-CM regulated macrophage polarization

We first investigated the effects of conditioned medium on macrophage polarization in normal myocytes or myoblasts in an inflammatory environment. LPS at 500 ng/mL and IL-4 at 20 ng/mL were utilized as a positive control, while the fresh exosome-depleted medium served as a negative control. We found that IF-CM and LPS induced M1 polarization (significantly more CD86+ cells compared with the control group), while NC-CM and IL-4 promoted M2 polarization (markedly more CD163+ cells compared with the control group) (Supplementary Figure 1). These results suggested that there was crosstalk between myoblasts and macrophages through their secretion. Therefore, we performed further experiments.

M1CM hindered myoblast myogenic differentiation

IF-C2C12 stimulated macrophages towards the M1 subtype for two days. Fresh medium was then added to the macrophages and 24 h later conditioned medium was collected to treat normal C2C12 (Supplementary Figure 2A). Giemsa stain and immunofluorescence results showed that the myotubes after M1CM administration were smaller and fewer than those of controls, which suggested that the myoblast myogenic differentiation ability was weakened by M1CM (Supplementary Figure 2B and C).

Identification and characterization of C2C12-Exos after LPS stimulation

Under transmission and SEM, C2C12-Exos appeared spherical or globular in shape (Figure 2A and B). Flow cytometry results demonstrated that exosomal markers (CD9, CD47, CD63, and CD81) were highly expressed in C2C12-Exos (Figure 2C). The NTA experiment evaluated the size of C2C12-Exos. The diameters ranged from 50-130 nm, which are consistent with the data from previous studies (Figure 2D). Western blot results showed that exosomal marker proteins (CD9, CD63, Alix, and HSP60) were highly expressed in C2C12-Exos, while these proteins were expressed in the exosome-depleted fractions (Figure 2E).

Exosomes tracing in vitro

To investigate how C2C12-Exos communicated with C2C12 and macrophages, C2C12-Exos were added to cultured C2C12 and RAW264.7 cells. PKH-67 (green) labeled C2C12-Exos were internalized into C2C12/macrophages and were identified in the cytoplasm after 12 h of co-culture. The Dye-only group showed no PKH67 signals (Figure 3A). The PKH-67 positivity rate was significantly higher in macrophages and C2C12 than in the Dye-only group (Figure 3B and C).

IF-C2C12-Exos induced M1 macrophage polarization *in vitro*

To examine the effects of IF-C2C12-Exos on macrophages, different concentrations of IF-C2C12-Exos were added to the culture system. After 48 h, as the concentration increased, the macrophages became more elongated and predominantly spindle-shaped compared with their original circular shape (Figure 4A). In addition, immunofluorescence staining showed an increase in CD86-positive cells and a decrease in CD206-positive cells as the concentration of IF-C2C12-Exos increased (Figure 4B). Moreover, flow cytometry results showed a significant increase in the proportion of M1 macrophages and a significant decrease in the proportion of M2 macrophages in the IF-C2C12-Exos group (Figure 4C-E). These data demonstrate that IF-C2C12-Exos induce the polarization of macrophages towards M1 *in vitro*.

IF-C2C12-Exos induced inflammatory reactions of macrophages *in vitro*

To further investigate the effects of IF-C2C12-Exos on macrophages, inflammatory-related factors were evaluated. The results of western blot demonstrated that IF-C2C12-Exos significantly up-regulated the protein expression (iNOS and CD86) and down-regulated that of CD206 and Arg1 (Figure 5A-D). In addition, immunofluorescence staining results showed that the relative expression and area of iNOS gradually increased with increasing concentrations of IF-C2C12-Exos (Figure 5E). Furthermore, ELISA results showed that the concentrations of cytokine IL-6, TNF- α , and IL-1 β in the culture supernatants significantly increased, while that of TGF- β did not show obvious changes after IF-C2C12-Exos treatment for 24 h (Figure 5F). Taken together, these data suggested that IF-C2C12-Exos can induce inflammatory reactions of macrophages *in vitro*.

IF-C2C12-Exos promoted C2C12 proliferation *in vitro*

To evaluate the effects of IF-C2C12-Exos on normal myoblasts, we first examined the proliferative capacity of the cells. The BrdU assay results showed that treatment with high concentrations of IF-C2C12-Exos (1×10^{10} , 2×10^{10} /medium) significantly increased the mean number of BrdU-positive cells, indicating that these C2C12 cells gained higher proliferation capacity (Figure 6A and C). Next, the wound-healing rate in the IF-C2C12-Exos group was significantly higher than that of the control group, which suggested that the migration capacity of C2C12 was enhanced by the IF-C2C12-Exos (Figure 6B and D). Furthermore, the results of the CCK-8 assay revealed a significant increase in the viability of C2C12 cells in the 2×10^{10} /medium concentration group after IF-C2C12-Exos treatment, while the low concentration group (1×10^9 , 1×10^{10}) showed a small but insignificant increase in viability (Figure 6E). Overall, these data demonstrate that IF-C2C12-Exos can stimulate normal C2C12 proliferation *in vitro*.

IF-C2C12-Exos impaired C2C12 differentiation *in vitro*

The fusion index of control myoblasts in differentiation and those treated with IF-C2C12-Exos were slightly different at the early stages (2 d) under all conditions tested (Figure 7A and B). More interestingly, after 4 d of differentiation, the fusion indices of the IF-C2C12-Exos treatment groups were significantly lower than that of the control group (14%-16% *vs* 32%) (Figure 8A and B).

In addition, our data also showed that myotube diameter and length were significantly affected by IF-C2C12-Exos treatments, with IF-C2C12-Exos inducing a significant decrease in myotube size at both early and late stages of muscle differentiation. As a result, there was a significant difference in the diameter and length of control and IF-C2C12-Exos myotubes, and this difference increased at higher IF-C2C12-Exos concentrations (Figures 7C-E and 8C-E). Finally, modulation of the myoblast fibrogenic/myogenic differentiation process in response to IF-C2C12-Exos treatment was investigated by western blot analysis. MyoG, MyoD1, MYHC, α -smooth muscle actin (SMA), and Col 1 protein expression levels showed a significant downregulation after 24 h of IF-C2C12-Exos treatment (Figure 9). Altogether, these data suggest that IF-C2C12-Exos impairs C2C12 muscle differentiation *in vitro* and triggers a shift in the balance of proliferation/differentiation towards proliferation.

DISCUSSION

This is the first study to demonstrate that myoblasts within the inflammatory environment crosstalk with surrounding macrophages. In this study, IF-C2C12-Exos

was shown to promote M1 polarization of M0 macrophages and to influence the balance of myoblast proliferation/differentiation *in vitro*.

Following acute mechanical injury, skeletal muscle develops significant inflammation[34,35]. If the M1 stage of macrophages persists after acute muscle injury, it will result in a prolonged inflammatory environment in the damaged area[14,36]. However, the underlying mechanism by which the M1 phenotype remains at the early and mid-stage of injury is less well understood. The similar appearance time of myoblasts and M1 macrophages after skeletal muscle injury may suggest a crosstalk between themselves[12,16]. CD86 and CD163 expression levels can reflect the polarization stage of macrophages[37]. In this study, the exosomes from inflammatory C2C12 myoblasts was found to induce higher levels of CD86 expression (M1 marker) than that of CD163 expression (M2 marker) in macrophages. Furthermore, we found that the inflammatory reactions in macrophages were also aggravated by IF-C2C12-Exos. A previous study[23] reported that exosomes from H₂O₂ treated myotubes could stimulate RAW264.7 macrophages to express higher levels of IL-6, which is consistent with our findings. However, we found other inflammatory factors, such as IL-1 β , TNF- α , and iNOS, were also upregulated in macrophage cultures following administration of high concentrations of IF-C2C12-Exos. This suggests that IF-C2C12-Exos may regulate macrophages to exert higher level inflammatory responses than those of H₂O₂-myotube-Exos. Interestingly, IF-C2C12-Exos reduced M2 macrophage expression, while IF-C2C12-CM did not exert that effect but also induced M1 polarization. Many studies have proved that macrophage polarization was regulated by surrounding environmental factors including cytokines and exosomes[38,39]. These results suggested that IF-C2C12-Exos can regulate the polarization of macrophages and maintain a prolonged inflammatory environment, while myoblasts in the inflammatory environment can continue to secrete IF-C2C12-Exos. This local positive feedback intercellular mechanism was observed in Xu *et al*[20]'s study, whereby C2C12-Exos promoted pre-osteoblasts differentiation to osteoblasts[20].

In this study, IF-C2C12-Exos were found to impair C2C12 differentiation and promote proliferation *in vitro*. In detail, decreased levels of MyoD, MyoG, and MYHC protein levels[25,26,40] suggesting that IF-C2C12-Exos reduced the myogenic differentiation ability of myoblasts. Induction experiments of myogenic differentiation also provided direct evidence for this result. In addition, the BrdU, CCK-8, and scratch assays[41] showed that a higher ability of myoblast proliferation was induced by IF-C2C12-Exos. This result is consistent with previous literature where exosomes from C2C12 myotube after H₂O₂ or TNF- α /interferon- γ treatment enhanced proliferation but impaired myogenic differentiation[23,42].

Significant and prolonged inflammation after acute muscle injury can result in muscle fibrosis[10,11,14,36]. Additionally, promoting M1 macrophages to M2 during the inflammatory phase after muscle injury prevents muscle fibrosis[27,43,44]. Interestingly, myocyte IF-C2C12-Exos treatment resulted in a significant decrease in protein levels of the fibrosis markers (Col 1, α -SMA), implying that the fibrogenic capacity of normal myoblasts was also suppressed[45]. We speculate that IF-C2C12-Exos are only secreted by myoblasts in the acute inflammatory stage (1-5 d after injury). They may disappear after day 5 due to inflammatory dissipation, meanwhile, M2 macrophages secrete a large amount of TGF- β , which activates myoblasts into fibroblasts, leading to ECM production[24,26,46]. However, due to prolonged inflammation caused by M1 macrophages, M2 polarization is incomplete and tissue remodeling is maladaptive, which leads to subsequent fibrosis[27,47]. Our results suggest that myoblasts passed information to surrounding myoblasts, telling them to grow faster but not differentiate under inflammatory conditions. This effect would have favored muscle regeneration, as large numbers of myoblasts are required to support muscle repair[48,49]. However, abnormal proliferation with down-regulated myogenic differentiation indeed hinders the muscle healing process after the acute inflammatory stage[50,51]. Additionally, the main effects of IF-C2C12-Exos are not to induce myoblast-derived fibrosis but to induce proliferation. A previous study proved that myoblasts are key in muscle fibrosis[52], and another study found that only promotion of myoblast proliferation cannot prevent fibrosis[6]. Therefore, we speculate that the IF-C2C12-Exos actually prepare the conditions for later fibrotic differentiation (accumulation of undifferentiated myogenic cells).

Together, the above results suggest that (1) IF-C2C12-Exos can induce macrophages towards M1 polarization, leading to a prolonged and aggravated inflammatory environment. In turn, the inflammatory factors stimulate myoblasts to produce more IF-C2C12-Exos, which forms a vicious circle; and (2) IF-C2C12-Exos can impair fibrogenic/myogenic differentiation, and lead to proliferation (Figure 10).

There are several limitations in this study that should be noted. First, we only utilized an *in vitro* model to study the effects of IF-C2C12-Exos on macrophages and myoblasts. However, muscle injury is a complex physiological and pathological issue with complex *in vivo* factors[53]. Further studies should consider validating the role of exosomes in animal models. Second, we only added IF-C2C12-Exos once; thus, multiple administrations should be considered, and the optimal concentration of exosomes should be studied in future research. Third, our study did not involve an in-depth mechanistic study. For example, myotubes were identified to promote myoblast fusion through exosomal miRNA[54]. Therefore, understanding the potential underlying mechanisms of how IF-C2C12-Exos can control macrophage polarization and influence the balance of myoblast proliferation/differentiation would be our future goal.

Given the pathophysiological significance of the findings of this study, further studies are needed to elucidate mechanisms responsible for these effects which deserve investigation. It is hoped that further studies will identify specific targets involved in muscle regeneration and fibrosis, such as lncRNAs and miRNAs.

CONCLUSION

Overall, this study demonstrates that IF-C2C12-Exos can promote M1 polarization and impair myoblasts differentiation. Normal or inflammatory myoblasts play a pivotal role, in fact, they release distinct Exos carrying a complex range of signals directed to the surrounding cells. Signals associated with Exos, by virtue of their diversity and specificity, may contribute to a fine reprogramming of the muscle regeneration process in a cooperative manner.

ARTICLE HIGHLIGHTS

Research background

More than half of sports injuries in athletes have been reported to be related to muscle damage. Severely injured muscles are prone to re-injury due to fibrotic scar formation caused by prolonged inflammation. How to regulate inflammation and suppress fibrosis is the focus of promoting muscle healing.

Research motivation

Recent studies have found that myoblasts and macrophages play important roles in the inflammatory phase following muscle injury; however, the crosstalk between these two types of cells in the inflammatory environment, particularly the exosome-related mechanisms, has not been well studied.

Research objectives

This study aimed to evaluate the effects of exosomes from inflammatory C2C12 myoblasts (IF-C2C12-Exos) on macrophage polarization and myoblast proliferation/differentiation.

Research methods

A model of inflammation was established *in vitro* by lipopolysaccharide stimulation of myoblasts. Multiple methods were used to isolate and identify the exosomes. Gradient concentrations of IF-C2C12-Exos were added to normal macrophages and myoblasts. PKH67 fluorescence tracing, microscopic morphology, Giemsa staining, immunofluorescence, ELISA assays, flow cytometry, western blot, BrdU test, scratch assay, and CCK-8 assay were conducted to determine the mechanism of IF-C2C12-Exos.

Research results

We found that the PKH-67-marked C2C12-Exos can be endocytosed by both macrophages and myoblasts. IF-C2C12-Exos induced M1 macrophage polarization and suppressed the M2 phenotype *in vitro*. These exosomes also stimulated the inflammatory reactions of macrophages. Furthermore, we demonstrated that IF-C2C12-Exos disrupted the balance of myoblast proliferation/differentiation, leading to enhanced proliferation and suppressed fibrogenic/myogenic differentiation.

Research conclusions

IF-C2C12-Exos can induce M1 polarization, resulting in a sustained and aggravated inflammatory environment that impairs myoblast differentiation, and leads to enhanced myogenic proliferation. These results demonstrate why prolonged inflammation occurs after acute muscle injury and provide a new target for the regulation of muscle regeneration.

Research perspectives

Given the pathophysiological significance of the findings of this study, further studies are needed to elucidate the mechanisms responsible for these effects which deserve investigation. It is hoped that further studies will identify specific targets involved in muscle regeneration and fibrosis, such as lncRNAs and miRNAs.

ACKNOWLEDGEMENTS

We are grateful to the Shanghai Institute of Nutrition and Health for providing the experimental platform.

REFERENCES

- 1 **Ekstrand J**, Hägglund M, Waldén M. Epidemiology of muscle injuries in professional football (soccer). *Am J Sports Med* 2011; **39**: 1226-1232 [PMID: 21335353 DOI: 10.1177/0363546510395879]
- 2 **Chiu CH**, Chang SS, Chang GJ, Chen AC, Cheng CY, Chen SC, Chan YS. The Effect of Hyperbaric Oxygen Treatment on Myoblasts and Muscles After Contusion Injury. *J Orthop Res* 2020; **38**: 329-335 [PMID: 31531986 DOI: 10.1002/jor.24478]
- 3 **Chiu CH**, Chang TH, Chang SS, Chang GJ, Chen AC, Cheng CY, Chen SC, Fu JF, Wen CJ, Chan YS. Application of Bone Marrow-Derived Mesenchymal Stem Cells for Muscle Healing After Contusion Injury in Mice. *Am J Sports Med* 2020; **48**: 1226-1235 [PMID: 32134689 DOI: 10.1177/0363546520905853]
- 4 **Beiner JM**, Jokl P. Muscle contusion injuries: current treatment options. *J Am Acad Orthop Surg* 2001; **9**: 227-237 [PMID: 11476532 DOI: 10.5435/00124635-200107000-00002]
- 5 **Mahdy MAA**. Skeletal muscle fibrosis: an overview. *Cell Tissue Res* 2019; **375**: 575-588 [PMID: 30421315 DOI: 10.1007/s00441-018-2955-2]
- 6 **Lieber RL**, Ward SR. Cellular mechanisms of tissue fibrosis. 4. Structural and functional consequences of skeletal muscle fibrosis. *Am J Physiol Cell Physiol* 2013; **305**: C241-C252 [PMID: 23761627 DOI: 10.1152/ajpcell.00173.2013]
- 7 **Bayer ML**, Bang L, Hoegberget-Kalisz M, Svensson RB, Olesen JL, Karlsson MM, Schjerling P, Hellsten Y, Hoier B, Magnusson SP, Kjaer M. Muscle-strain injury exudate favors acute tissue healing and prolonged connective tissue formation in humans. *FASEB J* 2019; **33**: 10369-10382 [PMID: 31211922 DOI: 10.1096/fj.201900542R]
- 8 **Zhang C**, Ferrari R, Beezhold K, Stearns-Reider K, D'Amore A, Haschak M, Stolz D, Robbins PD, Barchowsky A, Ambrosio F. Arsenic Promotes NF-Kb-Mediated Fibroblast Dysfunction and Matrix Remodeling to Impair Muscle Stem Cell Function. *Stem Cells* 2016; **34**: 732-742 [PMID: 26537186 DOI: 10.1002/stem.2232]
- 9 **Zhao L**, Liu X, Zhang J, Dong G, Xiao W, Xu X. Hydrogen Sulfide Alleviates Skeletal Muscle Fibrosis via Attenuating Inflammation and Oxidative Stress. *Front Physiol* 2020; **11**: 533690 [PMID: 33071808 DOI: 10.3389/fphys.2020.533690]
- 10 **Prabhu SD**, Frangogiannis NG. The Biological Basis for Cardiac Repair After Myocardial Infarction: From Inflammation to Fibrosis. *Circ Res* 2016; **119**: 91-112 [PMID: 27340270 DOI: 10.1161/CIRCRESAHA.116.303577]
- 11 **Zhang M**, Jiang SK, Tian ZL, Wang M, Zhao R, Wang LL, Li SS, Liu M, Li JY, Zhang MZ, Guan DW. CB2R orchestrates fibrogenesis through regulation of inflammatory response during the repair of skeletal muscle contusion. *Int J Clin Exp Pathol* 2015; **8**: 3491-3502 [PMID: 26097533]
- 12 **Moyer AL**, Wagner KR. Regeneration vs fibrosis in skeletal muscle. *Curr Opin Rheumatol* 2011; **23**: 568-573 [DOI: 10.1097/bor.0b013e32834bac92]
- 13 **Martins L**, Gallo CC, Honda TSB, Alves PT, Stilhano RS, Rosa DS, Koh TJ, Han SW. Skeletal muscle healing by M1-like macrophages produced by transient expression of exogenous GM-CSF. *Stem Cell Res Ther* 2020; **11**: 473 [PMID: 33158459 DOI: 10.1186/s13287-020-01992-1]
- 14 **Wynn TA**, Vannella KM. Macrophages in Tissue Repair, Regeneration, and Fibrosis. *Immunity* 2016; **44**: 450-462 [PMID: 26982353 DOI: 10.1016/j.immuni.2016.02.015]
- 15 **Sass FA**, Fuchs M, Pumberger M, Geissler S, Duda GN, Perka C, Schmidt-Bleek K. Immunology Guides Skeletal Muscle Regeneration. *Int J Mol Sci* 2018; **19** [PMID: 29534011 DOI: 10.3390/ijms19030835]

- 16 **Tidball JG**, Villalta SA. Regulatory interactions between muscle and the immune system during muscle regeneration. *Am J Physiol Regul Integr Comp Physiol* 2010; **298**: R1173-R1187 [PMID: 20219869 DOI: 10.1152/ajpregu.00735.2009]
- 17 **Kang H**, Lee MJ, Park SJ, Lee MS. Lipopolysaccharide-Preconditioned Periodontal Ligament Stem Cells Induce M1 Polarization of Macrophages through Extracellular Vesicles. *Int J Mol Sci* 2018; **19** [PMID: 30513870 DOI: 10.3390/ijms19123843]
- 18 **Song M**, Han L, Chen FF, Wang D, Wang F, Zhang L, Wang ZH, Zhong M, Tang MX, Zhang W. Adipocyte-Derived Exosomes Carrying Sonic Hedgehog Mediate M1 Macrophage Polarization-Induced Insulin Resistance via Pthc and PI3K Pathways. *Cell Physiol Biochem* 2018; **48**: 1416-1432 [PMID: 30064125 DOI: 10.1159/000492252]
- 19 **Gao F**, Zuo B, Wang Y, Li S, Yang J, Sun D. Protective function of exosomes from adipose tissue-derived mesenchymal stem cells in acute kidney injury through SIRT1 pathway. *Life Sci* 2020; **255**: 117719 [PMID: 32428599 DOI: 10.1016/j.lfs.2020.117719]
- 20 **Xu Q**, Cui Y, Luan J, Zhou X, Li H, Han J. Exosomes from C2C12 myoblasts enhance osteogenic differentiation of MC3T3-E1 pre-osteoblasts by delivering miR-27a-3p. *Biochem Biophys Res Commun* 2018; **498**: 32-37 [PMID: 29476741 DOI: 10.1016/j.bbrc.2018.02.144]
- 21 **Théry C**, Witwer KW, Aikawa E, Alcaraz MJ, Anderson JD, Andriantsitohaina R, Antoniou A, Arab T, Archer F, Atkin-Smith GK, Ayre DC, Bach JM, Bachurski D, Baharvand H, Balaj L, Baldacchino S, Bauer NN, Baxter AA, Bebawy M, Beckham C, Bedina Zavec A, Benmoussa A, Berardi AC, Bergese P, Bielska E, Blenkiron C, Bobis-Wozowicz S, Boilard E, Boireau W, Bongiovanni A, Borràs FE, Bosch S, Boulanger CM, Breakefield X, Breglio AM, Brennan MÁ, Brigstock DR, Brisson A, Broekman ML, Bromberg JF, Bryl-Górecka P, Buch S, Buck AH, Burger D, Busatto S, Buschmann D, Bussolati B, Buzás EI, Byrd JB, Camussi G, Carter DR, Caruso S, Chamley LW, Chang YT, Chen C, Chen S, Cheng L, Chin AR, Clayton A, Clerici SP, Cocks A, Cocucci E, Coffey RJ, Cordeiro-da-Silva A, Couch Y, Coumans FA, Coyle B, Crescitelli R, Criado MF, D'Souza-Schorey C, Das S, Datta Chaudhuri A, de Candia P, De Santana EF, De Wever O, Del Portillo HA, Demaret T, Deville S, Devitt A, Dhondt B, Di Vizio D, Dieterich LC, Dolo V, Dominguez Rubio AP, Dominici M, Dourado MR, Driedonks TA, Duarte FV, Duncan HM, Eichenberger RM, Ekström K, El Andaloussi S, Elie-Caille C, Erdbrügger U, Falcón-Pérez JM, Fatima F, Fish JE, Flores-Bellver M, Försönits A, Frelet-Barrand A, Fricke F, Fuhrmann G, Gabrielsson S, Gámez-Valero A, Gardiner C, Gärtner K, Gaudin R, Gho YS, Giebel B, Gilbert C, Gimona M, Giusti I, Goberdhan DC, Görgens A, Gorski SM, Greening DW, Gross JC, Gualerzi A, Gupta GN, Gustafson D, Handberg A, Haraszti RA, Harrison P, Hegyesi H, Hendrix A, Hill AF, Hochberg FH, Hoffmann KF, Holder B, Holthofer H, Hosseinkhani B, Hu G, Huang Y, Huber V, Hunt S, Ibrahim AG, Ikezu T, Inal JM, Isin M, Ivanova A, Jackson HK, Jacobsen S, Jay SM, Jayachandran M, Jenster G, Jiang L, Johnson SM, Jones JC, Jong A, Jovanovic-Talisman T, Jung S, Kalluri R, Kano SI, Kaur S, Kawamura Y, Keller ET, Khamari D, Khomyakova E, Khvorova A, Kierulf P, Kim KP, Kislinger T, Klingeborn M, Klinke DJ 2nd, Kornek M, Kosanović MM, Kovács ÁF, Krämer-Albers EM, Krasemann S, Krause M, Kurochkin IV, Kusuma GD, Kuypers S, Laitinen S, Langevin SM, Languino LR, Lannigan J, Lässer C, Laurent LC, Lavie G, Lázaro-Ibáñez E, Le Lay S, Lee MS, Lee YXF, Lemos DS, Lenassi M, Leszczynska A, Li IT, Liao K, Libregts SF, Ligeti E, Lim R, Lim SK, Linē A, Linnemannstons K, Llorente A, Lombard CA, Lorenowicz MJ, Lőrincz ÁM, Lötval J, Lovett J, Lowry MC, Loyer X, Lu Q, Lukomska B, Lunavat TR, Maas SL, Malhi H, Marcilla A, Mariani J, Mariscal J, Martens-Uzunova ES, Martin-Jaular L, Martínez MC, Martins VR, Mathieu M, Mathivanan S, Mauerer M, McGinnis LK, McVey MJ, Meckes DG Jr, Meehan KL, Mertens I, Minciacchi VR, Möller A, Möller Jørgensen M, Morales-Kastresana A, Morhayim J, Mullier F, Muraca M, Musante L, Mussack V, Muth DC, Myburgh KH, Najrana T, Nawaz M, Nazarenko I, Nejsum P, Neri C, Neri T, Nieuwland R, Nimrichter L, Nolan JP, Nolte-t Hoen EN, Noren Hooten N, O'Driscoll L, O'Grady T, O'Loughlin A, Ochiya T, Olivier M, Ortiz A, Ortiz LA, Osteikoetxea X, Østergaard O, Ostrowski M, Park J, Pegtel DM, Peinado H, Perut F, Pfaffl MW, Phinney DG, Pieters BC, Pink RC, Pisetsky DS, Pogge von Strandmann E, Polakovicova I, Poon IK, Powell BH, Prada I, Pulliam L, Quesenberry P, Radeghieri A, Raffai RL, Raimondo S, Rak J, Ramirez MI, Raposo G, Rayaan MS, Regev-Rudzki N, Ricklefs FL, Robbins PD, Roberts DD, Rodrigues SC, Rohde E, Rome S, Rouschop KM, Ruggetti A, Russell AE, Saá P, Sahoo S, Salas-Huenuleo E, Sánchez C, Saugstad JA, Saul MJ, Schifferers RM, Schneider R, Schøyen TH, Scott A, Shahaj E, Sharma S, Shatnyeva O, Shekari F, Shelke GV, Shetty AK, Shiba K, Siljander PR, Silva AM, Skowronek A, Snyder OL 2nd, Soares RP, Sódar BW, Soekmadji C, Sotillo J, Stahl PD, Stoorvogel W, Stott SL, Strasser EF, Swift S, Tahara H, Tewari M, Timms K, Tiwari S, Tixeira R, Tkach M, Toh WS, Tomasini R, Torrecilhas AC, Tosar JP, Toxavidis V, Urbanelli L, Vader P, van Balkom BW, van der Grein SG, Van Deun J, van Herwijnen MJ, Van Keuren-Jensen K, van Niel G, van Royen ME, van Wijnen AJ, Vasconcelos MH, Vechetti IJ Jr, Veit TD, Vella LJ, Velot É, Verweij FJ, Vestad B, Viñas JL, Visnovitz T, Vukman KV, Wahlgren J, Watson DC, Wauben MH, Weaver A, Webber JP, Weber V, Wehman AM, Weiss DJ, Welsh JA, Wendt S, Wheelock AM, Wiener Z, Witte L, Wolfram J, Xagorari A, Xander P, Xu J, Yan X, Yáñez-Mó M, Yin H, Yuana Y, Zappulli V, Zarubova J, Žekas V, Zhang JY, Zhao Z, Zheng L, Zheutlin AR, Zickler AM, Zimmermann P, Zivkovic AM, Zocco D, Zuba-Surma EK. Minimal information for studies of extracellular vesicles 2018 (MISEV2018): a position statement of the International Society for Extracellular Vesicles and update of the MISEV2014 guidelines. *J Extracell Vesicles* 2018; **7**: 1535750 [PMID: 30637094 DOI: 10.1080/20013078.2018.1535750]
- 22 **Huang C**, Luo WF, Ye YF, Lin L, Wang Z, Luo MH, Song QD, He XP, Chen HW, Kong Y, Tang

- YK. Characterization of inflammatory factor-induced changes in mesenchymal stem cell exosomes and sequencing analysis of exosomal microRNAs. *World J Stem Cells* 2019; **11**: 859-890 [PMID: 31692888 DOI: 10.4252/wjsc.v11.i10.859]
- 23 **Guescini M**, Maggio S, Ceccaroli P, Battistelli M, Annibalini G, Piccoli G, Sestili P, Stocchi V. Extracellular Vesicles Released by Oxidatively Injured or Intact C2C12 Myotubes Promote Distinct Responses Converging toward Myogenesis. *Int J Mol Sci* 2017; **18** [PMID: 29165341 DOI: 10.3390/ijms18112488]
- 24 **Sun Y**, Wang H, Li Y, Liu S, Chen J, Ying H. miR-24 and miR-122 Negatively Regulate the Transforming Growth Factor- β /Smad Signaling Pathway in Skeletal Muscle Fibrosis. *Mol Ther Nucleic Acids* 2018; **11**: 528-537 [PMID: 29858088 DOI: 10.1016/j.omtn.2018.04.005]
- 25 **Lin J**, Luo Z, Liu S, Chen Q, Chen J. Long non-coding RNA H19 promotes myoblast fibrogenesis via regulating the miR-20a-5p-Tgfb2 axis. *Clin Exp Pharmacol Physiol* 2021; **48**: 921-931 [PMID: 33615521 DOI: 10.1111/1440-1681.13489]
- 26 **Lin J**, Yang X, Liu S, Luo Z, Chen Q, Sun Y, Ding Z, Chen J. Long non-coding RNA MFAT1 promotes skeletal muscle fibrosis by modulating the miR-135a-5p-Tgfb2/Smad4 axis as a ceRNA. *J Cell Mol Med* 2021; **25**: 4420-4433 [PMID: 33837645 DOI: 10.1111/jcmm.16508]
- 27 **Luo Z**, Lin J, Sun Y, Wang C, Chen J. Bone Marrow Stromal Cell-Derived Exosomes Promote Muscle Healing Following Contusion Through Macrophage Polarization. *Stem Cells Dev* 2021; **30**: 135-148 [PMID: 33323007 DOI: 10.1089/scd.2020.0167]
- 28 **Shokrollahi E**, Nourazarian A, Rahbarghazi R, Salimi L, Karbasforush S, Khaksar M, Salarinasab S, Abhari A, Heidarzadeh M. Treatment of human neuroblastoma cell line SH-SY5Y with HSP27 siRNA tagged-exosomes decreased differentiation rate into mature neurons. *J Cell Physiol* 2019; **234**: 21005-21013 [PMID: 31012118 DOI: 10.1002/jcp.28704]
- 29 **Woo CH**, Kim HK, Jung GY, Jung YJ, Lee KS, Yun YE, Han J, Lee J, Kim WS, Choi JS, Yang S, Park JH, Jo DG, Cho YW. Small extracellular vesicles from human adipose-derived stem cells attenuate cartilage degeneration. *J Extracell Vesicles* 2020; **9**: 1735249 [PMID: 32284824 DOI: 10.1080/20013078.2020.1735249]
- 30 **Sharma AK**, Hota PV, Matoka DJ, Fuller NJ, Jandali D, Thaker H, Ameer GA, Cheng EY. Urinary bladder smooth muscle regeneration utilizing bone marrow derived mesenchymal stem cell seeded elastomeric poly(1,8-octanediol-co-citrate) based thin films. *Biomaterials* 2010; **31**: 6207-6217 [PMID: 20488535 DOI: 10.1016/j.biomaterials.2010.04.054]
- 31 **Sato S**, Basse AL, Schönke M, Chen S, Samad M, Altıntaş A, Laker RC, Dalbram E, Barrès R, Baldi P, Trebak JT, Zierath JR, Sassone-Corsi P. Time of Exercise Specifies the Impact on Muscle Metabolic Pathways and Systemic Energy Homeostasis. *Cell Metab* 2019; **30**: 92-110.e4 [PMID: 31006592 DOI: 10.1016/j.cmet.2019.03.013]
- 32 **Sun Y**, Chen W, Hao Y, Gu X, Liu X, Cai J, Liu S, Chen J, Chen S. Stem Cell-Conditioned Medium Promotes Graft Remodeling of Midsubstance and Intratunnel Incorporation After Anterior Cruciate Ligament Reconstruction in a Rat Model. *Am J Sports Med* 2019; **47**: 2327-2337 [PMID: 31306585 DOI: 10.1177/0363546519859324]
- 33 **Chen W**, Sun Y, Gu X, Cai J, Liu X, Zhang X, Chen J, Hao Y, Chen S. Conditioned medium of human bone marrow-derived stem cells promotes tendon-bone healing of the rotator cuff in a rat model. *Biomaterials* 2021; **271**: 120714 [PMID: 33610048 DOI: 10.1016/j.biomaterials.2021.120714]
- 34 **Kobayashi M**, Ota S, Terada S, Kawakami Y, Otsuka T, Fu FH, Huard J. The Combined Use of Losartan and Muscle-Derived Stem Cells Significantly Improves the Functional Recovery of Muscle in a Young Mouse Model of Contusion Injuries. *Am J Sports Med* 2016; **44**: 3252-3261 [PMID: 27501834 DOI: 10.1177/0363546516656823]
- 35 **Xiao W**, Liu Y, Luo B, Zhao L, Liu X, Zeng Z, Chen P. Time-dependent gene expression analysis after mouse skeletal muscle contusion. *J Sport Health Sci* 2016; **5**: 101-108 [PMID: 30356928 DOI: 10.1016/j.jshs.2016.01.017]
- 36 **Li Q**, Zheng M, Liu Y, Sun W, Shi J, Ni J, Wang Q. A pathogenetic role for M1 macrophages in peritoneal dialysis-associated fibrosis. *Mol Immunol* 2018; **94**: 131-139 [PMID: 29306153 DOI: 10.1016/j.molimm.2017.12.023]
- 37 **Xu HT**, Lee CW, Li MY, Wang YF, Yung PS, Lee OK. The shift in macrophages polarisation after tendon injury: A systematic review. *J Orthop Translat* 2020; **21**: 24-34 [PMID: 32071872 DOI: 10.1016/j.jot.2019.11.009]
- 38 **Pritchard A**, Tousif S, Wang Y, Hough K, Khan S, Strenkowski J, Chacko BK, Darley-Usmar VM, Deshane JS. Lung Tumor Cell-Derived Exosomes Promote M2 Macrophage Polarization. *Cells* 2020; **9** [PMID: 32456301 DOI: 10.3390/cells9051303]
- 39 **Davis MJ**, Tsang TM, Qiu Y, Dayrit JK, Freij JB, Huffnagle GB, Olszewski MA. Macrophage M1/M2 polarization dynamically adapts to changes in cytokine microenvironments in *Cryptococcus neoformans* infection. *mBio* 2013; **4**: e00264-e00213 [PMID: 23781069 DOI: 10.1128/mBio.00264-13]
- 40 **Xu D**, Wang L, Jiang Z, Zhao G, Hassan HM, Sun L, Fan S, Zhou Z, Zhang L, Wang T. A new hypoglycemic mechanism of catalpol revealed by enhancing MyoD/MyoG-mediated myogenesis. *Life Sci* 2018; **209**: 313-323 [PMID: 30118770 DOI: 10.1016/j.lfs.2018.08.028]
- 41 **Wei X**, Li H, Zhang B, Li C, Dong D, Lan X, Huang Y, Bai Y, Lin F, Zhao X, Chen H. miR-378a-3p promotes differentiation and inhibits proliferation of myoblasts by targeting HDAC4 in skeletal muscle development. *RNA Biol* 2016; **13**: 1300-1309 [PMID: 27661135 DOI: 10.1080/15476286.2016.1239008]

- 42 **Kim S**, Lee MJ, Choi JY, Park DH, Kwak HB, Moon S, Koh JW, Shin HK, Ryu JK, Park CS, Park JH, Kang JH. Roles of Exosome-Like Vesicles Released from Inflammatory C2C12 Myotubes: Regulation of Myocyte Differentiation and Myokine Expression. *Cell Physiol Biochem* 2018; **48**: 1829-1842 [PMID: 30092568 DOI: 10.1159/000492505]
- 43 **Stout RD**, Jiang C, Matta B, Tietzel I, Watkins SK, Suttles J. Macrophages sequentially change their functional phenotype in response to changes in microenvironmental influences. *J Immunol* 2005; **175**: 342-349 [PMID: 15972667 DOI: 10.4049/jimmunol.175.1.342]
- 44 **Qiu X**, Liu S, Zhang H, Zhu B, Su Y, Zheng C, Tian R, Wang M, Kuang H, Zhao X, Jin Y. Mesenchymal stem cells and extracellular matrix scaffold promote muscle regeneration by synergistically regulating macrophage polarization toward the M2 phenotype. *Stem Cell Res Ther* 2018; **9**: 88 [PMID: 29615126 DOI: 10.1186/s13287-018-0821-5]
- 45 **Li Y**, Foster W, Deasy BM, Chan Y, Prisk V, Tang Y, Cummins J, Huard J. Transforming growth factor-beta1 induces the differentiation of myogenic cells into fibrotic cells in injured skeletal muscle: a key event in muscle fibrogenesis. *Am J Pathol* 2004; **164**: 1007-1019 [PMID: 14982854 DOI: 10.1016/s0002-9440(10)63188-4]
- 46 **Liu X**, Long X, Liu W, Zhao Y, Hayashi T, Yamato M, Mizuno K, Fujisaki H, Hattori S, Tashiro SI, Ogura T, Atsuzawa Y, Ikejima T. Type I collagen induces mesenchymal cell differentiation into myofibroblasts through YAP-induced TGF-β1 activation. *Biochimie* 2018; **150**: 110-130 [PMID: 29777737 DOI: 10.1016/j.biochi.2018.05.005]
- 47 **Nakagawa M**, Karim MR, Izawa T, Kuwamura M, Yamate J. Immunophenotypical Characterization of M1/M2 Macrophages and Lymphocytes in Cisplatin-Induced Rat Progressive Renal Fibrosis. *Cells* 2021; **10** [PMID: 33525592 DOI: 10.3390/cells10020257]
- 48 **Yin H**, Price F, Rudnicki MA. Satellite cells and the muscle stem cell niche. *Physiol Rev* 2013; **93**: 23-67 [PMID: 23303905 DOI: 10.1152/physrev.00043.2011]
- 49 **Zhao Y**, Chen M, Lian D, Li Y, Wang J, Deng S, Yu K, Lian Z. Non-Coding RNA Regulates the Myogenesis of Skeletal Muscle Satellite Cells, Injury Repair and Diseases. *Cells* 2019; **8** [PMID: 31461973 DOI: 10.3390/cells8090988]
- 50 **Perandini LA**, Chimin P, Lutkemeyer DDS, Câmara NOS. Chronic inflammation in skeletal muscle impairs satellite cells function during regeneration: can physical exercise restore the satellite cell niche? *FEBS J* 2018; **285**: 1973-1984 [PMID: 29473995 DOI: 10.1111/febs.14417]
- 51 **Sorensen JR**, Kaluhiokalani JP, Hafen PS, Deyhle MR, Parcell AC, Hyldahl RD. An altered response in macrophage phenotype following damage in aged human skeletal muscle: implications for skeletal muscle repair. *FASEB J* 2019; **33**: 10353-10368 [PMID: 31208207 DOI: 10.1096/fj.201900519R]
- 52 **Brack AS**, Conboy MJ, Roy S, Lee M, Kuo CJ, Keller C, Rando TA. Increased Wnt signaling during aging alters muscle stem cell fate and increases fibrosis. *Science* 2007; **317**: 807-810 [PMID: 17690295 DOI: 10.1126/science.1144090]
- 53 **Huard J**, Li Y, Fu FH. Muscle injuries and repair: current trends in research. *J Bone Joint Surg Am* 2002; **84**: 822-832 [PMID: 12004029]
- 54 **Forterre A**, Jalabert A, Berger E, Baudet M, Chikh K, Errazuriz E, De Larichaudy J, Chanon S, Weiss-Gayet M, Hesse AM, Record M, Geloën A, Lefai E, Vidal H, Couté Y, Rome S. Proteomic analysis of C2C12 myoblast and myotube exosome-like vesicles: a new paradigm for myoblast-myotube cross talk? *PLoS One* 2014; **9**: e84153 [PMID: 24392111 DOI: 10.1371/journal.pone.0084153]



Published by **Baishideng Publishing Group Inc**
7041 Koll Center Parkway, Suite 160, Pleasanton, CA 94566, USA
Telephone: +1-925-3991568
E-mail: bpgoffice@wjgnet.com
Help Desk: <https://www.f6publishing.com/helpdesk>
<https://www.wjgnet.com>

